

VCBART: Bayesian trees for varying coefficients

Sameer K. Deshpande*, Ray Bai†, Cecilia Balocchi‡,
Jennifer E. Starling§ and Jordan Weiss¶

February 23, 2022

Abstract

Many studies have reported associations between later-life cognition and socioeconomic position in childhood, young adulthood, and mid-life. However, the vast majority of these studies are unable to quantify how these associations vary over time and with respect to several demographic factors. Varying coefficient (VC) models, which treat the covariate effects in a linear model as nonparametric functions of additional effect modifiers, offer an appealing way to overcome these limitations. Unfortunately, state-of-the-art VC modeling methods require computationally prohibitive parameter tuning or make restrictive assumptions about the functional form of the covariate effects.

In response, we propose VCBART, which estimates the covariate effects in a VC model using Bayesian Additive Regression Trees. With simple default hyperparameter settings, VCBART outperforms existing methods in terms of covariate effect estimation and prediction. Using VCBART, we predict the cognitive trajectories of 4,167 subjects from the Health and Retirement Study using multiple measures of socioeconomic position and physical health. We find that socioeconomic position in childhood and young adulthood have small effects that do not vary with age. In contrast, the effects of measures of mid-life physical health tend to vary with respect to age, race, and marital status. An R package implementing VC-BART is available at <https://github.com/skdeshpande91/VCBART>

*UW–Madison. sameer.deshpande@wisc.edu

†Department of Statistics, University of South Carolina

‡Department of Economics and Statistics, University of Torino

§Mathematica Policy Research

¶Department of Demography, University of California, Berkeley

1 Introduction

1.1 Socioeconomic position and cognition

A large body of evidence suggests that socioeconomic position (SEP) at different points in the life course is an important determinant of cognitive function as well as its underlying risk factors in mid-life and older adulthood (Luo and Waite, 2005; Lyu and Burr, 2016; Marden et al., 2017; Greenfield and Moorman, 2019; Zhang et al., 2020). For instance, financial resources during childhood (Marden et al., 2017), educational attainment (Seblova et al., 2020) in early adulthood, and occupational complexity (Jorm et al., 1998) have all been associated with cognitive function and decline. A critical open challenge in life course research is to estimate how the association between cognitive function and SEP at different stages of life evolve over time and with respect to other sociodemographic characteristics. Because it can help identify risk factors that predispose some people to poor cognitive health later in life, addressing this challenge has important public health implications, in light of a rapidly aging population.

To date, however, while several existing papers attempt to estimate time-varying effects of different measures of SEP on cognition, the vast majority impose strong parametric assumptions about the functional form of these effects. For instance, despite the merits of their work, both Lyu and Burr (2016) and Marden et al. (2017) assume that the effect of childhood SEP on cognition evolves linearly with age, which may not be the case for all individuals. Such structural assumptions are made not because of substantive prior belief about the effect in question. Rather, they are typically made out of computational convenience. Additionally, most existing empirical works linking cognitive function to SEP fail to examine whether and how the temporal evolution of these links may vary with respect to key socio-demographic factors. In this paper, we address these methodological limitations by fitting a flexible linear varying coefficient (VC) model to longitudinal data from the US-based Health and Retirement Study (HRS).

1.2 The challenges of varying coefficient modeling

VC modeling begins by specifying a set of p covariates, which we denote by X , and a set of R effect modifiers, which we denote by Z , and modeling

$$Y = \beta_0(Z) + \beta_1(Z)X_1 + \cdots + \beta_p(Z)X_p + \varepsilon \tag{1}$$

where the $\beta_0(Z), \dots, \beta_p(Z)$ are *functions* mapping \mathbb{R}^R to \mathbb{R} and the residual error ε has mean zero.

Our dataset consists of a total of $N = 27,844$ longitudinal observations of $n = 4,167$ HRS subjects. In our particular application, we focus on predicting each subject’s total score on a battery of cognitive assessments administered biennially between 2000 and 2016. To do this, we fit a VC model whose covariates X include measures of SEP in childhood, early adulthood, and later-life as well as measures of later-life physical and mental health. To allow for covariate effects to vary across time and across the population, our set of modifiers Z include age and several socio-demographic factors like race, birth place, marital status, food stamp status, and labor force status. In fitting our VC model, we have several desiderata. First, in sharp contrast to the models considered by [Lyu and Burr \(2016\)](#) and [Marden et al. \(2017\)](#), we wish to make minimal assumptions about the functional form of the covariate effects $\beta_j(Z)$. Additionally, we wish to identify which elements of Z actually modify the effects of which elements of X . Given the potential public health implications of carefully estimating heterogeneous effects, we further require calibrated and coherent uncertainty quantification for both covariate effects $\beta_j(Z)$ and forecasted cognitive trajectories. Finally, we require a method that can scale to the size of our dataset.

1.3 Our contributions

Unfortunately, to the best of our knowledge, no existing procedure for fitting VC models meets all of our desiderata of flexibility, uncertainty quantification, and scalability. To wit, existing state-of-the-art procedures with multivariate modifiers either involve learning a large number of tuning parameters using leave-one-out cross-validation or rigidly assume that the covariate effects $\beta_j(Z)$ are additive in Z . Moreover, the default implementations of existing procedures do not provide any out-of-sample, *predictive* uncertainty quantification.

We instead propose approximating each covariate effect function $\beta_j(Z)$ with a sum of shallow piecewise constant regression trees, effectively extending [Chipman et al. \(2010\)](#)’s Bayesian Additive Regression Tree (BART) model to the VC setting. On synthetic data, we demonstrate that our proposed extension, which we call **VCBART**, exhibits superior covariate effect recovery compared to the current state-of-the-art *without computationally intensive hand-tuning or imposing strong structural assumptions*. Moreover, compared to more flexible blackbox regression procedures, VCBART can provide substantially more interpretable fits to data without sacrificing predictive power. We finally show that, under mild conditions,

the VCBART posterior concentrates at a near-optimal rate, even with correlated residual errors. To the best of our knowledge, our Theorem 1 is the first result to demonstrate the theoretical near-optimality of Bayesian treed regression in settings with non-i.i.d. noise. Applying VCBART to our HRS dataset, we found that by the time subjects in our study population reached older adulthood, the effects of SEP in childhood and early adulthood were essentially constant over time. We also found that, in our dataset, diabetics displayed consistently worse cognitive functioning than non-diabetics. Interestingly, however, amongst diabetic subjects, those who were married had slightly better cognitive functioning than those who were unmarried.

Here is an outline for the rest of the paper. We briefly review relevant background on VC modeling, BART, and the HRS dataset in Section 2. Then, in Section 3, we introduce VCBART, describe how to perform posterior inference, and state our asymptotic results. In Section 4, we demonstrate VCBART’s excellent covariate effect recovery and predictive capabilities using synthetic data. We finally apply VCBART to the HRS data in Section 5 and outline several avenues for future work in Section 6.

2 Background

2.1 Limitations of existing work linking SEP & cognition

Over the past several decades, researchers have explored the link between life course SEP and later-life cognitive function. Their goal was to understand how life course processes unfold to shape trajectories of cognitive and physical health. Several, but not all, studies have reported that childhood SEP is an important determinant of cognitive function in older adulthood. Moreover, the accumulation of low SEP at multiple stages of the life course may produce the greatest deficits to cognitive health.

In order to model the time-varying effects of SEP covariates, several authors augment a simple linear model with interactions between the SEP covariates and functions of age. For instance, both [Marden et al. \(2017\)](#) and [Lyu and Burr \(2016\)](#) include interactions between age and SEP covariates. These models are essentially linear VC models whose covariate effects are linear functions of a single modifier (age). While these models are easy to fit, these specifications may not be well-suited to capture more complex temporal dynamics. For instance, while there may be a strong associations between educational attainment (a commonly used proxy for SEP in early adulthood) and several health outcomes in early

adulthood and mid-life, these association can weaken, diminish, and level off as people age (see Dupre (2007) and references therein). Such trends cannot be captured by a simple linear function. While some authors like Aartsen et al. (2019) introduce an additional interaction between SEP covariates and age-squared, it is not clear whether these models are flexible enough to detect more complex non-linear relationships.

2.2 The HRS dataset

We use publicly available data from the Health and Retirement Study (HRS). The HRS is a nationally representative longitudinal survey of US adults over the age of 50 and their spouses of any age. Since 1992, the HRS has biennially assessed the economic, health, and social implications of aging through its core survey with response rates greater than 85% in each wave. The HRS is sponsored by the National Institute on Aging (NIA; U01AG009740) and is conducted by the University of Michigan. See Sonnega et al. (2014) for additional details about the HRS.

In each wave, the HRS consistently administered a battery of cognitive tests that include tasks like listening to a series of 10 words and recalling as many possible immediately and several minutes later. The HRS constructed a summary score that ranges from 0 to 35, with higher scores reflecting better cognitive functioning. In our analysis, we use the total cognitive score as our outcome.

Our covariate set includes measures of SEP at three distinct stages of life and physical health in older adulthood. We used a composite childhood SEP index developed and validated by Vable et al. (2017). This index is based on the educational attainment and occupation of each subject’s parents and their overall financial well-being in childhood. Higher scores on this index correspond to higher SEP. We used total years of education as a proxy for SEP in early adulthood and household wealth in 1998 as a proxy for later-life SEP. Our later-life physical and mental health covariates, which were all recorded in 1998, include binary indicators of diabetes, heart problems, high blood pressure, loneliness, participation in regular physical activity, and stroke. Since body mass index (BMI; Dahl et al. (2013)) and depression (Lichtenberg et al., 1995) have been negatively associated with later-life cognition, we include BMI and score on the Center for Epidemiological Studies – Depression scale (CES-D) as covariates. The CES-D scale counts the number of depressive symptoms a subject experiences in a week.

To estimate how the effects of our covariates might vary over time and across several socio-

demographic factors, our set of modifiers included age, gender, race, birthplace, veteran status, marital status, labor force status, and indicators of whether or not respondents were food insecure or received food stamps in 1998. We additionally included self-reported childhood health as a potential modifier. After expanding each multi-level categorical modifier into binary dummy variables, we had a total of $R = 16$ potential modifiers. Table 1 lists all of the covariate and modifiers used in our analysis.

2.3 Varying Coefficient Models

Since their introduction in [Hastie and Tibshirani \(1993\)](#), VC models have been extensively studied and deployed in both the statistics and econometrics literature. We give a very brief overview here and refer the reader to [Fan and Zhang \(2008\)](#) and [Franco-Villoria et al. \(2019\)](#) for more comprehensive reviews.

When there is only a single modifier (i.e. $R = 1$), one popular approach (see, e.g., [Hoover et al. \(1998\)](#) and [Huang et al. \(2002\)](#)) is to express each β_j as a linear combination of pre-specified basis functions. Such a decomposition effectively reduces the functional regression problem to a high-dimensional linear regression problem for which numerous frequentist (see, e.g. [Wang et al., 2008](#); [Wang and Xia, 2009](#); [Wei et al., 2011](#)) and Bayesian ([Bai et al., 2019](#)) regularization techniques have been proposed. Kernel smoothing is another popular and theoretically supported alternative (see, e.g., [Wu and Chiang, 2000](#)).

In spatial statistics, the β_j 's are typically modeled with Gaussian processes (see, e.g., [Gelfand et al. \(2003\)](#) and [Finley and Banerjee \(2020\)](#)) to allow covariate effects to vary smoothly in time and space. When the number of observations is large, full Bayesian inference with Markov Chain Monte Carlo (MCMC) can be computationally prohibitive. Recently, [Guhaniyogi et al. \(2020\)](#) proposed a distributed computing strategy to spatially-varying coefficient models using Gaussian processes.

Outside the context of spatial models, to accommodate models with multivariate modifiers, [Tibshirani and Friedman \(2019\)](#) and [Lee et al. \(2018\)](#) respectively constrained the covariate effects to be linear and additive functions of the potential modifiers. In contrast, [Li and Racine \(2010\)](#) proposed a multivariate kernel smoothing estimator that imposes no rigid structural assumptions on the β_j 's. However, the default implementation of their procedure tunes several bandwidth parameters with leave-one-out cross-validation. When n , p , or R are large, as in our analysis, kernel smoothing is computationally prohibitive.

In the last decade, several authors have proposed using regression trees to estimate the covariate effects $\beta_j(Z)$. [Bürgin and Ritschard \(2015\)](#), for instance, model each $\beta_j(Z)$ with a single regression tree while [Wang and Hastie \(2012\)](#) and [Zhou and Hooker \(2019\)](#) both use boosting to construct separate ensembles for each $\beta_j(Z)$. Although trees are an intuitively appealing approach, existing procedures require substantial tuning and do not provide non-asymptotic out-of-sample uncertainty quantification.

2.4 Bayesian Additive Regression Trees

We now briefly describe BART. To set our notation, let T denote a binary decision tree partitioning \mathbb{R}^R that consists of a collection of interior nodes and $L(T)$ terminal or *leaf* nodes. We associate an axis-aligned decision rule of the form $\{Z_v < c\}$ to each internal (i.e. non-leaf) node of T . These decision rules are determined by the pair (v, c) of splitting variable index v and cut-point c . The $L(T)$ leaves of T partition \mathbb{R}^R into rectangular cells and we let $\ell(\mathbf{z}; T)$ be the function that returns the index of the leaf containing the point \mathbf{z} . A *regression tree* is a pair $(T, \boldsymbol{\mu})$ consisting of a decision tree T and collection of *jumps* $\boldsymbol{\mu} = \{\mu_1, \dots, \mu_{L(T)}\}$ associated with each leaf of T . The evaluation function $g(\mathbf{z}; T, \boldsymbol{\mu}) = \mu_{\ell(\mathbf{z}; T)}$ returns the jump corresponding to the leaf containing \mathbf{z} .

In the standard nonparametric regression problem $y = f(\mathbf{z}) + \epsilon$, [Chipman et al. \(2010\)](#) approximated the unknown f with a sum of M *a priori* independent regression trees

$$f(\mathbf{z}) \approx \sum_{m=1}^M g(\mathbf{z}; T_m, \boldsymbol{\mu}_m).$$

Priors over the regression trees $(T_m, \boldsymbol{\mu}_m)$ were then updated to compute an approximate posterior over f . The regression tree prior consisted of two parts, a branching process prior over the decision tree T_m and a conditionally Gaussian prior over the jumps $\boldsymbol{\mu}_m | T_m$. The branching process prior can be described in three parts: (i) the probability that a node at depth d is non-terminal, (ii) a distribution for selecting the splitting variable index v used at each non-terminal node, and (iii) a distribution for selecting the cutpoint $c|v$ at each internal decision node. Posterior inference in the basic BART model is performed using a Metropolis-within-Gibbs sampler that sequentially updates each individual regression tree while keeping the others fixed. Each regression tree update involves first drawing a new decision tree T'_m with a Metropolis-Hastings step and then updating the jumps $\boldsymbol{\mu}_m$ conditionally given the new decision tree. The new decision tree T'_m is drawn from a transition kernel that randomly

grows or prunes the existing decision tree. See [Pratola \(2016\)](#) for a more detailed discussion of MH proposals for regression trees.

The basic BART model has been extended successfully to survival analysis ([Sparapani et al., 2016](#)), multiple imputation ([Xu et al., 2016](#)), log-linear models ([Murray, 2019](#)), semi-continuous responses ([Linerio et al., 2019](#)), and causal inference ([Hill, 2011](#); [Hahn et al., 2020](#)). BART has also been modified to recover smooth ([Linerio and Yang, 2018](#); [Starling et al., 2019b](#)) and monotonic ([Chipman et al., 2019](#); [Starling et al., 2019a](#)) functions. In each of these settings, new BART-based methods often substantially outperform existing state-of-the-art procedures in terms of function recovery and prediction. Moreover, recent results in [Ročková and van der Pas \(2019\)](#) and [Ročková and Saha \(2019\)](#) demonstrate BART’s theoretical near-optimality under very mild assumptions. We refer the reader to [Tan and Roy \(2019\)](#) for a more detailed review of BART and its many extensions.

3 The VCBART Procedure

For each subject $i = 1, \dots, n$, we observe n_i triplets $(\mathbf{x}_{it}, \mathbf{z}_{it}, y_{it})$ of covariates, modifiers, and outcome at time points $t = t_{i1}, \dots, t_{in_i}$. For all $i = 1, \dots, n$, and $t = 1, \dots, n_i$, we model

$$y_{it} = \beta_0(\mathbf{z}_{it}) + \sum_{j=1}^p \beta_j(\mathbf{z}_{it})x_{itj} + \sigma\varepsilon_{it}. \quad (2)$$

Since the HRS dataset consists of repeated measurements of each subject, we assume $\boldsymbol{\varepsilon}_i = (\varepsilon_{i1}, \dots, \varepsilon_{in_i})^\top \sim \mathcal{N}(\mathbf{0}_{n_i}, \boldsymbol{\Sigma}_i(\rho))$ where $\boldsymbol{\Sigma}_i(\rho)$ is a correlation matrix with off-diagonal elements equal to $0 \leq \rho < 1$. We assume that the noise vectors $\boldsymbol{\varepsilon}_i$ ’s are independent across subjects. We do not assume that we observe each subject an equal number of times nor do we assume that the observation times are equally spaced.

The key idea of VCBART is to approximate each covariate effect $\beta_j(\mathbf{z})$ with its own ensemble of *a priori* i.i.d. regression trees $\mathcal{E}_j = \{(T_m^{(j)}, \boldsymbol{\mu}_m^{(j)})\}_{m=1}^M$,

$$\beta_j(\mathbf{z}) \approx \sum_{m=1}^M g(\mathbf{z}; T_m^{(j)}, \boldsymbol{\mu}_m^{(j)}).$$

We place independent and identical priors on the individual regression trees $(T_m^{(j)}, \boldsymbol{\mu}_m^{(j)})$. Like [Chipman et al. \(2010\)](#), we place a branching process prior on the decision trees $T_m^{(j)}$ and

model $\boldsymbol{\mu}_j^{(m)} | T_m^{(j)} \sim \mathcal{N}(\mathbf{0}_{L(T_m^{(j)})}, \tau_j^2 I_{L(T_m^{(j)})})$ where $\tau_j > 0$ is fixed. We set the prior probability that a node at depth d is non-terminal to be $0.95(1+d)^{-2}$, thereby placing substantial prior probability on trees of depth less than five.

For each $j = 1, \dots, p$, and $r = 1, \dots, R$, let θ_{jr} be the prior probability that Z_r is selected as the splitting variable in a decision rule in the ensemble \mathcal{E}_j . Let $\boldsymbol{\theta}_j = (\theta_{j1}, \dots, \theta_{jR})$. Whereas [Chipman et al. \(2010\)](#) drew the splitting index v at each internal node uniformly (i.e. each $\theta_{jr} = 1/R$), we follow [Linero \(2018\)](#) and adaptively learn these probabilities. To this end, we model $\boldsymbol{\theta}_j \sim \text{Dirichlet}(\eta_j/R, \dots, \eta_j/R)$ and place a further discrete prior over $\eta_j/(\eta_j + R)$. This prior hierarchy encourages sparsity in the set of splitting variables used in each ensemble \mathcal{E}_j . Conditionally on the splitting index v , we pick the cutpoint c uniformly. We complete our prior specification with a half- t_ν prior on σ^2 .

For a fixed autocorrelation ρ , we use a straightforward extension of [Chipman et al. \(2010\)](#)'s basic sampler to simulate posterior draws. Conditionally on all other parameters, we sequentially update each of the $M(p+1)$ regression trees by first drawing a new decision tree with an MH step and then conditionally updating the jumps. After updating every regression tree, we update σ with an additional MH step. Like [Linero \(2018\)](#), we update each $\boldsymbol{\theta}_j$ with a Dirichlet–Multinomial conjugate update. We defer the full derivation of our sampler to [Section S2](#). An R package implementing VCBART is also available at <https://github.com/skdeshpande91/VCBART>.

Although it is tempting to place a further prior on the autocorrelation ρ and add an additional Gibbs step to our sampler, we have found that the conditional posterior of ρ is extremely concentrated around its current value, resulting in very slow mixing. As a result, like [Hoover et al. \(1998\)](#), we do not attempt to model ρ jointly with the other parameters. Instead, in practice, we recommend setting ρ with cross-validation.

Modifier selection. In our sampler, in order to update the vector of splitting index probabilities $\boldsymbol{\theta}_j$, we keep track of the number of times each modifier Z_r is used in a decision rule in the ensemble \mathcal{E}_j . Using these counts, we can estimate probability that each Z_r is selected at least once in the ensemble \mathcal{E}_j used to estimate β_j . These selection probabilities are directly analogous to the posterior inclusion probabilities encountered in Bayesian sparse linear regression. Based on this interpretation, for each ensemble \mathcal{E}_j , we construct an analog of [Barbieri and Berger \(2004\)](#)'s median probability model by reporting those modifiers Z_r whose selection probability exceeds 0.5.

Asymptotic Results. To facilitate a theoretical analysis of VCBART, we assume that the R modifiers have been rescaled to lie in $[0, 1]^R$ and that there are true functions $\beta_{0,0}, \dots, \beta_{0,p}$ satisfying

$$y_{it} = \beta_{0,0}(\mathbf{z}_{it}) + \sum_{j=0}^p \beta_{0,j}(\mathbf{z}_{it})x_{itj} + \sigma_0 \varepsilon_{it}, \quad i = 1, \dots, n, t = 1, \dots, n_i, \quad (3)$$

where each function $\beta_{0,j}$ is α_j -Hölder continuous with $0 < \alpha_j \leq 1$, and $\boldsymbol{\varepsilon}_i = (\varepsilon_{i1}, \dots, \varepsilon_{in_i})^\top \sim \mathcal{N}(\mathbf{0}_{n_i}, \boldsymbol{\Sigma}_i(\rho_0))$. With minor modifications to the decision tree prior, the VCBART posterior concentrates around the true function values at the near-optimal rate as the total number of observations grows to infinity.

Let $N = \sum_{i=1}^n n_i$ be the total number of observations across all n subjects, and let $\boldsymbol{\beta}$ and $\boldsymbol{\beta}_0$ be $N \times (p+1)$ matrices whose respective (i, j) -th entries are $\beta_j(\mathbf{z}_{it})$ and $\beta_{0,j}(\mathbf{z}_{it})$. Let $\|\boldsymbol{\beta} - \boldsymbol{\beta}_0\|_N^2 = N^{-1} \sum_{i=1}^n \sum_{t=1}^{n_i} \sum_{j=0}^p [\beta_j(\mathbf{z}_{it}) - \beta_{0,j}(\mathbf{z}_{it})]^2$ be the squared empirical ℓ_2 norm. If we knew the true smoothness level α_j of each β_j , the minimax-optimal rate for estimating $\boldsymbol{\beta}_0$ in $\|\cdot\|_N^2$ norm would be $r_N^2 = \sum_{j=0}^p N^{-2\alpha_j/(2\alpha_j+R)}$ (Ročková and van der Pas, 2019). In the absence of this knowledge, Theorem 1 shows that VCBART can estimate the varying coefficients $\boldsymbol{\beta}_0$ at nearly this rate, sacrificing only a logarithmic factor.

Theorem 1. *Under (3), suppose we endow $(\boldsymbol{\beta}, \sigma)$ with a modified VCBART prior, where the splitting probability of each node at depth d in a decision tree is given by γ^d , for some $N^{-1} \leq \gamma < 0.5$ and the splitting indices are chosen uniformly (i.e. $\boldsymbol{\theta} = (1/R, \dots, 1/R)$), and $\nu > 1$ in the half- t_ν prior on σ . Suppose we further endow ρ with the uniform prior, $\rho \sim \mathcal{U}(0, 1)$. Assume that assumptions (A1)-(A4) in Section S4 hold. Then for some constant $M > 0$ and $r_N^2 = \log N \sum_{j=0}^p N^{-2\alpha_j/(2\alpha_j+R)}$,*

$$\Pi(\boldsymbol{\beta} : \|\boldsymbol{\beta} - \boldsymbol{\beta}_0\|_N > Mr_N | \mathbf{Y}) \rightarrow 0, \quad (4)$$

in $\mathbb{P}_{\boldsymbol{\beta}_0}^{(N)}$ -probability as $N, p \rightarrow \infty$.

The proof of Theorem 1 is in Section S4.

4 Simulation Studies

In this section, we demonstrate the application of VCBART on a synthetic data set. First, we compare VCBART's ability to recover the covariate effect functions $\beta_j(Z)$ with several

other VC methods. We continue with a comparison of the predictive performance of VC-BART and several blackbox procedures. We finally assess VCBART’s ability to identify which elements of Z modify the effects of which elements of X .

Our synthetic dataset consisted of $p = 5$ correlated covariates and $R = 20$ potential effect modifiers. The correlated covariates were drawn from a multivariate normal distribution with mean zero and a covariance matrix with entries $0.75^{|i-j|}$. The modifiers were drawn uniformly from the interval $[0, 1]$. To demonstrate the performance of VCBART in the presence of both continuous and discrete modifiers, we discretized Z_2 and Z_{16}, \dots, Z_{20} based on whether or not they exceeded 0.5. We generated $n_i = 4$ observations for $n = 500$ subjects from the model in (2) with $\sigma = 1$ and the following covariate effect functions:

$$\begin{aligned} \beta_0(\mathbf{z}) &= 3z_1 + (2 - 5z_2) \sin(\pi z_1) - 2z_2 \\ \beta_1(\mathbf{z}) &\sim \text{GP}(0, K); K(\mathbf{z}, \mathbf{z}') = 2 \exp \left\{ -\frac{(z_1 - z_1')^2}{2(0.05)^2} - \frac{2}{(0.1)^2} \sin \left(\frac{\pi(z_1 - z_1')^2}{4} \right) \right\} \\ \beta_2(\mathbf{z}) &= (3 - 3z_1^2 \cos(6\pi z_1)) \times \mathbf{1}(z_1 > 0.6) - 10\sqrt{z_1} \times \mathbf{1}(z_1 < 0.25) \\ \beta_3(\mathbf{z}) &= (1 - z_3)^{\frac{1}{3}} \sin(3\pi(1 - z_4)) - \sqrt{1 - z_1} \\ \beta_4(\mathbf{z}) &= 10 \sin(\pi z_1 z_2) + 20(z_3 - 0.5)^2 + 10z_4 + 5z_5 \\ \beta_5(\mathbf{z}) &= \exp \left\{ \sin \left((0.9(z_1 + 0.48))^{10} \right) \right\} + z_2 z_3 + z_4. \end{aligned}$$

The functions β_4 and β_5 were studied by [Friedman \(1991\)](#) and [Gramacy and Lee \(2009\)](#).

The top row of [Figure 1](#) shows the functions β_0, \dots, β_3 . The bottom row of [Figure 1](#) superimposes the VCBART posterior mean and 95% credible intervals for β_0, \dots, β_3 computed using the full synthetic dataset over the true functions. The posterior mean and uncertainty bands were computed after running two independent chains of VCBART for 1,500 iterations, discarding the first 500 samples of each as burn-in. We approximated each β_j with an ensemble of $M = 50$ trees and set each $\tau_j = M^{-\frac{1}{2}}$. While this is a somewhat arbitrary choice for τ_j , we have found that it works well in practice and defer a more detailed hyperparameter sensitivity analysis to [Section S2](#).

Although the covariate effect functions we considered had markedly different shapes, VCBART recovered each remarkably well: the posterior means of each β_j closely tracked the shape of the true functions and, for the most part, the true function values were within the shaded pointwise 95% credible intervals.

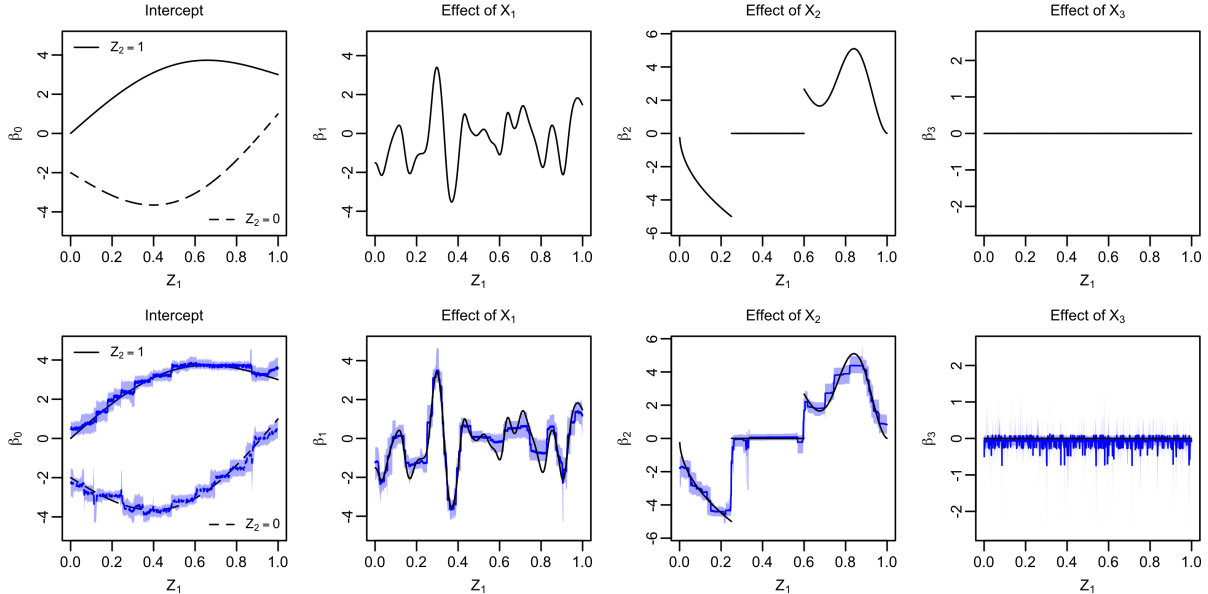


Figure 1: **Top row.** True functions β_0, \dots, β_3 . **Bottom row.** VCBART's posterior mean (blue line) and pointwise 95% credible interval (shaded) for each function

Covariate effect recovery. We compared VCBART's out-of-sample covariate effect recovery performance to that of the standard linear model (implemented using the function `lm` in R), Li and Racine (2010)'s kernel smoothing (KS; implemented in the `np` package by Hayfield and Racine (2008)), Bürgin and Ritschard (2015)'s TVCM procedure (implemented in the `vcrpart` package (Bürgin and Ritschard, 2017)), and Zhou and Hooker (2019)'s boosted tree procedure method (BTVCM; R code available at <https://github.com/siriuz42/treeboostVCM>). Because KS and TVCM involved substantial tuning with cross-validation, we compared all of these methods using 75 randomly drawn training subjects and 25 randomly drawn testing subjects. Figure 2(a) compares the out-of-sample mean square error (MSE) averaged over all six functions and over all 100 testing set observations across 25 different training–testing subsets. VCBART produced much more accurate point estimates of the $\beta_j(\mathbf{z})$'s than its competitors. It is interesting to note that KS often returned worse out-of-sample estimates of $\beta_j(\mathbf{z})$ than the standard linear model.

We also compared the frequentist coverage of VCBART's 95% credible intervals for the covariate effects with the 95% confidence intervals produced by the competitors. Since the off-the-shelf implementations of KS, TVCM, and BTVCM do not return standard errors of the estimated covariate effects, we formed 95% bootstrap confidence intervals. Although there is no *a priori* reason to expect that the VCBART 95% posterior credible intervals for

the $\beta_j(\mathbf{z})$'s will have 95% frequentist coverage, it is encouraging to see in Figure 2(b) that the coverage was above 80%. Furthermore, the VCBART credible intervals were consistently shorter than the bootstrap intervals for KS, TVCM, and BTVCM. It also took substantially less time to run VCBART (5 minutes) than to run KS (34 min.), TVCM (86 min.), and BTVCM (60 min.) with 50 bootstrap replications. We report function-by-function performance in Section S3.

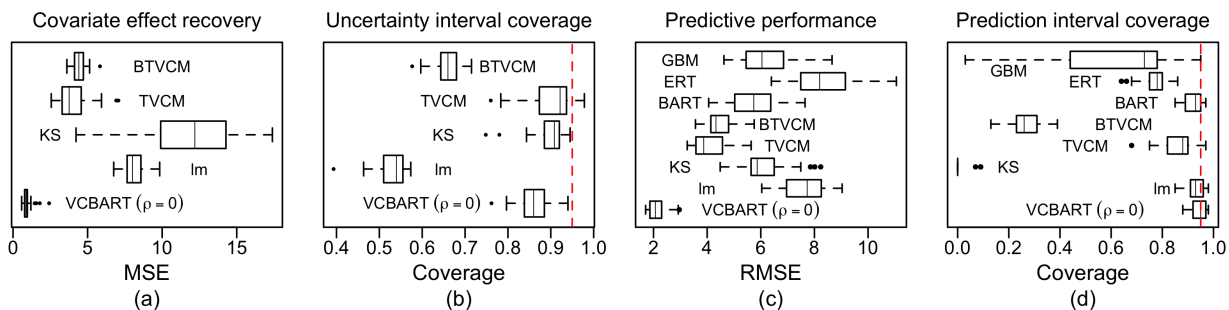


Figure 2: (a) Total mean square error for estimating β_j . (b) Frequentist coverage of 95% uncertainty intervals for $\beta_j(\mathbf{z})$. (c) Out-of-sample predictive root mean square error. (d) Coverage of 95% prediction intervals. All measures reported over 25 training–testing splits.

Predictive performance. We also compared VCBART’s predictive performance to those of blackbox procedures like BART (implemented in the `BART` R package by McCulloch et al. (2018)), extremely randomized trees (ERT; implemented in the `ranger` R package by Wright and Ziegler (2017)), and gradient boosting machines (GBM; implemented in the `gbm` R package by Greenwell et al. (2019)). Figures 2(c) and (d) compare the out-of-sample root mean square error (RMSE) and coverage of the 95% prediction intervals.

On our synthetic dataset, TVCM, BTVCM, and VCBART had substantially smaller out-of-sample RMSEs than the blackbox methods (BART, ERT, and GBM), despite the latter methods being more flexible. We moreover found that VCBART consistently achieved the smallest predictive RMSE in all of our simulations and produced prediction intervals with close to the nominal 95% coverage. While BTVCM and GBM sometimes produced prediction intervals that were much shorter than VCBART’s, these intervals tended to have much less than nominal coverage. Further, although BART generally produced prediction intervals with similar coverage as VCBART, we found that VCBART’s prediction intervals were, on average, about three times shorter than BART’s. Interestingly, in nearly all simulations, KS overfit the training data, resulting in in-sample RMSEs several orders of magnitude smaller than those of other methods and prediction intervals with essentially zero coverage.

Modifier selection. In the previous section, we described how to construct a median probability model to identify the modifiers Z_r on which each function β_j depends. The average sensitivity, specificity, precision, and accuracy of our median probability model, averaged across all functions β_j and across the 25 training–testing splits, were 0.81, 0.96, 0.75, and 0.95. These results indicate relatively promising modifier selection.

5 Analysis of the HRS Data

We restricted our analysis to HRS subjects who were dementia-free in 1998 and who had at least two cognitive scores recorded between 2000 and 2016. This resulted in an analytic sample of $n = 4,167$ subjects who contributed a total of $N = 27,844$ person-years over the study period. The average age of subjects in 1998 was 66.58 years. Each subject contributed between four and eight observations to our sample. Table 1 lists all of the covariates and potential modifiers included in our analysis.

Table 1: Covariates and potential modifiers used in our analysis. The column MPM reports the median probability model estimated for each covariate.

Variable	Description	MPM
cSES	Vable et al. (2017) ’s childhood SEP index.	\emptyset
education	Educational attainment in years. Proxy for early adulthood SEP	race, food_stamp
wealth	Household wealth in 1998. Proxy for later-life SEP	\emptyset
CESD	Score on CES-D scale for depression in 1998.	age
BMI	Body mass index in 1998.	age
phy_act	Participated in regular physical activity in 1998.	age
diab	Diagnosed with diabetes in 1998 or earlier.	age, marital
hi_bp	Diagnosed with high blood pressure or hypertension by 1998.	age, race
heart	Diagnosed with heart problems in 1998 or earlier.	age, race
stroke	Suffered at least one stroke by 1998.	southern
lonely	Experienced loneliness in by 1998.	age
age	Age in months (modifier)	
chld_hlth	Self-rated childhood health (modifier)	
race	Race (modifier; 4 levels)	
gender	Gender (modifier)	
southern	Whether subject was born in Southern U.S. (modifier)	
foreign	Whether subject was born outside the U.S. (modifier)	
veteran	Whether subject was veteran (modifier)	
marital	Marital status in 1998 (modifier)	
labor	Labor force status in 1998 (modifier; 3 levels)	
food_stamp	Whether subject received food stamps in 1998 (modifier)	
food_insec	Whether subject experienced food insecurity in 1998 (modifier)	

Predictive performance. Figure 3 compares the out-of-sample predictive performance

and the coverage of the 95% prediction intervals of VCBART and the competing methods studied in the previous section across 25 75%-25% training-testing splits of our HRS dataset. Because KS and TVCM did not converge within eight hours, their performances were excluded from our comparison. We see clearly that for several values of ρ , VCBART achieved smaller RMSEs than the competing methods. In fact, in all 25 of our simulations, VCBART with $\rho = 0.5$ had smaller RMSE than each of the blackbox methods (BART, ERT, and GBM).

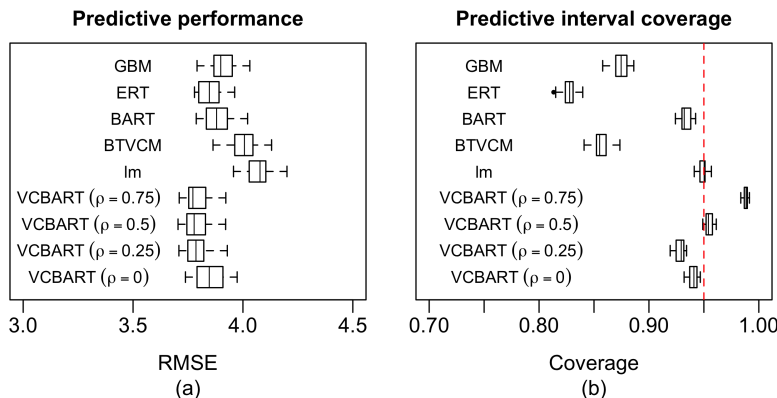


Figure 3: (a) Out-of-sample root mean square error. (b) Coverage of 95% prediction intervals. All measures reported over 25 75%-25% training-testing splits.

Modifier selection. In order to determine which modifiers drive heterogeneity in which covariate effects, we ran VCBART with $\rho = 0.5$ on the entire dataset and formed the median probability model for each β_j as described in Section 3. The median probability model for each covariate effect function is reported in Table 1. Interestingly, none of our three measures of SEP (childhood SEP index, education, and baseline wealth) displayed age-varying effects. In fact, the effect of education only varied with respect to race and food stamp status in 1998. Additionally, we found that the effect of diabetes varied with respect to both age and marital status in 1998.

Estimated varying coefficients. Figure 4 plots the posterior mean and 95% credible intervals of the effects of several covariates across the life-course for two hypothetical individuals. Both individuals were Southern-born men who rated their health as generally excellent in childhood and who were working full-time in 1998. The individual whose effects are plotted in blue was white and unmarried in 1998 while the individual whose effects are plotted in red was black and married in 1998. The dashed vertical lines in each panel show the 5%

and 95% quantiles of the distribution of ages in our dataset. As one would expect, there is considerably more uncertainty about the estimated effects outside of this age range.

In Figure 4(a), we not only see that the white male’s estimated intercept (shown in blue) is larger than the black male’s (shown in red), but also that the white male’s intercept decreases at a much faster rate between the ages of 65 and 90. This finding is consistent with previous literature that reports race-varying rates of cognitive decline (Wilson et al., 2015; Díaz-Venegas et al., 2016).

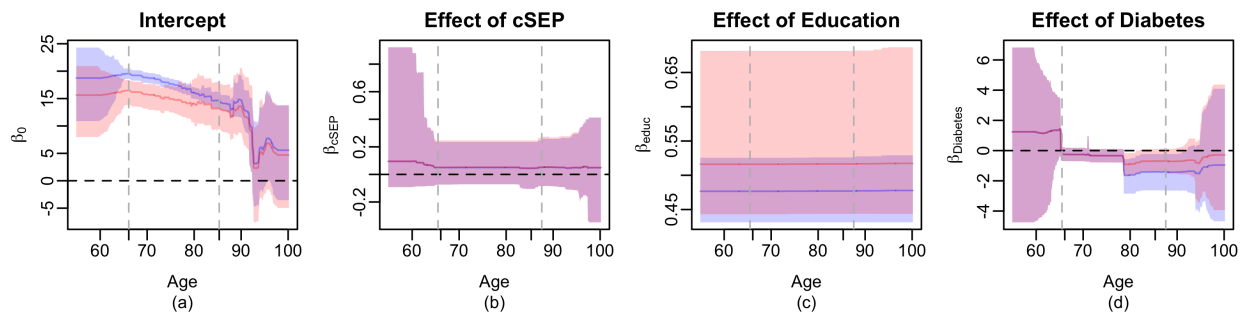


Figure 4: Posterior mean and 95% credible intervals (shaded) of the effects of several covariates for two hypothetical individuals, an unmarried white male (blue) and a married black male (red). The dashed vertical lines are located at the 5% and 95% quantiles of the distribution of ages in our dataset.

Figure 4(b) suggests that the effect of childhood SEP on later-life cognition is essentially constant in older adulthood. Indeed, for both individuals shown in Figure 4, a unit change in Vable et al. (2017)’s childhood SEP index was associated with an increase of about 0.05 in cognitive score. In our full dataset, the posterior mean effects of childhood SEP ranged from -0.06 to 0.12. These estimated effects were all considerably smaller than 4.36, the overall standard deviation of cognitive scores, which themselves ranged from 0 to 35. We additionally found that for each person in our dataset, the 95% credible intervals of this effect contained both positive and negative values. Our results suggest that by the time subjects reach older adulthood, childhood SEP has relatively little predictive effect on later-life cognition, after accounting for later-life physical health and other SEP measures.

Consistent with the median probability model reported in Table 1, Figure 4(c) shows that the effect of educational attainment was essentially constant throughout older adulthood. In contrast with childhood SEP, every individual’s 95% credible intervals for the effect of education contained only positive values. This finding is consistent with a large body of

literature that reports a protective effect of higher educational attainment. However, these credible intervals contained predominantly small values and the overwhelming majority of our posterior samples were between 0.2 and 0.9. In other words, while an additional year of education was associated with an increased cognitive score, the associated increase was typically less than a point.

In Figure 4(d), we see that prior to age 66, which is around the 5% quantile of ages in our dataset, there is considerable uncertainty about the effect of diabetes. However, between ages 66 and 85 (i.e. the middle 90% of ages in our dataset), we found that, after adjusting for the other covariates, subjects with diabetes had worse cognitive scores than those without diabetes. As reported in Table 1, according to our median probability model, the effect of diabetes was modified only by age and marital status. Interestingly, we found that the estimated effects for the married (red) and unmarried (blue) individuals were virtually indistinguishable until about age 80, at which point the estimated effect for the married individual is slightly smaller in magnitude. This finding is consistent with studies that have shown marriage or cohabitation may mediate lifestyle behaviors and diabetes management and may improve health outcomes (Beverly et al., 2008; Liu et al., 2016).

6 Discussion

We have introduced VCBART for fitting linear varying coefficient models that retain the interpretability of linear models while displaying predictive accuracy on par with more flexible, blackbox regression models. On simulated data, VCBART displayed covariate effect function recovery and predictive performance superior to existing state-of-the-art VC methods *without intensive problem-specific tuning or imposing any structural assumptions about the functions $\beta_j(Z)$* . It moreover returned coherent and generally well-calibrated uncertainty quantifications. Theorem 1 shows that the VCBART posterior concentrates at close to the minimax optimal rate, losing only a logarithmic factor.

We used VCBART to predict the cognitive trajectories of 4,167 subjects from the Health and Retirement Study using a combination of demographic, physical health, and socio-economic variables. We found that by the time that subjects in our dataset reached older adulthood, the effects of childhood SEP and educational attainment were quite small and essentially constant over time. In line with a broader literature, we found that among respondents with diabetes, those who were married had slightly better cognitive outcomes than those who

were unmarried.

Although it is well established that higher educational attainment corresponds to better cognitive performance on average (Seblova et al., 2020), some prior studies have reported that more formal education may not correspond to linear trajectories of cognitive decline (Wilson et al., 2009; Zahodne et al., 2011; Piccinin et al., 2013; Gross et al., 2015; Sisco et al., 2015). Instead, allowing for nonlinearity in the effect of education on cognitive decline over time may better capture the dynamics of the life course (Wilson et al., 2009). Even then, however, associations between education and cognitive decline have been reported to vary with respect to other variables which are seldom jointly studied (see, e.g., Wilson et al. (2009)). Taken together, the results obtained from our study are consistent with and extend a broader literature seeking to identify life course determinants of cognitive function and decline.

In our analysis, we did not explicitly adjust for potential selection biases and confounding. Indeed, it is possible that subjects with higher childhood SEP tended to be better educated and more well-off in later-life. For a more rigorous study of causal effects of SEP on cognitive trajectories, similar to Marden et al. (2017), we could use inverse-probability weights. Incorporating observation-specific weights to the basic VCBART algorithm is relatively straightforward. Relatedly, the Bayesian causal forest models of Hahn et al. (2020) and Woody et al. (2020) are special cases of our more general VCBART model with single covariate. It would be interesting to study VCBART’s ability to estimate the simultaneous effects of multiple, possibly continuous, treatments under suitable identifying assumptions.

Throughout this work we have assumed that the sets of covariates X and effect modifiers Z was fixed and known. While domain knowledge and theory often suggest natural choices of effect modifiers, we can readily envision scenarios in which it is not immediately clear whether a particular predictor should enter Equation (1) as a covariate, modifier, or both. In these situations, we recommend setting both X and Z equal to the full set of available predictors.

7 Acknowledgements

The third listed author was supported by the European Research Council (ERC) under the European Union’s Horizon 2020 research and innovation programme under grant agreement No. 817257.”

References

- Aartsen, M. J., Cheval, B., Sieber, S., Van der Linden, B. W., Gabriel, R., Courvoisier, D. S., Guessous, I., Burton-Jeangros, C., Blane, D., Ihle, A., Kliegel, M., and Cullati, S. (2019). Advantaged socioeconomic conditions in childhood are associated with higher cognitive functioning but strong cognitive decline in older age. *Proceedings of the National Academy of Sciences*, 116(2):5478 – 5486.
- Bai, R., Boland, M. R., and Chen, Y. (2019). Fast algorithms and theory for high-dimensional Bayesian varying coefficient models. arXiv:1907.06477.
- Barbieri, M. M. and Berger, J. O. (2004). Optimal predictive model selection. *Annals of Statistics*, 32(3):870 – 897.
- Beverly, E., Wray, L. A., and Miller, C. K. (2008). Practice implications of what couples tell us about type 2 diabetes management. *Diabetes Spectrum*, 21(1):39–45.
- Bürgin, R. and Ritschard, G. (2015). Tree-based varying coefficient regression for longitudinal ordinal responses. *Computational Statistics and Data Analysis*, 86:65 – 80.
- Bürgin, R. and Ritschard, G. (2017). Coefficient-wise tree-based varying coefficient regression with verpart. *Journal of Statistical Software*, 80(6):1 – 33.
- Chipman, H. A., George, E. I., and McCulloch, R. E. (2010). BART: Bayesian additive regression trees. *Annals of Applied Statistics*, 4(1):266 – 298.
- Chipman, H. A., George, E. I., McCulloch, R. E., and Shively, T. S. (2019). High-dimensional nonparametric monotone function estimation using BART. arXiv:1612.01619v2.
- Dahl, A. K., Hassing, L. B., Fransson, E. I., Gatz, M., Reynolds, C. A., and Pedersen, N. L. (2013). Body mass index across midlife and cognitive change in late life. *International Journal of Obesity*, 37(2):296 – 302.
- Díaz-Venegas, C., Downer, B., Langa, K. M., and Wong, R. (2016). Racial and ethnic differences in cognitive function among older adults in the USA. *International Journal of Geriatric Psychiatry*, 31(9):1004 – 1012.
- Dupre, M. E. (2007). Educational differences in age-related patterns of disease: Reconsidering the cumulative disadvantage and age-as-leveler hypotheses. *Journal of Health and Social Behavior*, 48(1):1 – 15.

- Eddelbuettel, D. and François, R. (2011). Rcpp: Seamless R and C++ integration. *Journal of Statistical Software*, 40(8):1 – 18.
- Eddelbuettel, D. and Sanderson, C. (2014). Rcpparmadillo: Accelerating R with high-performance C++ linear algebra. *Computational Statistics and Data Analysis*, 71:1054 – 1063.
- Fan, J. and Zhang, W. (2008). Statistical methods with varying coefficient models. *Statistics and its Interface*, 1:179 – 195.
- Finley, A. O. and Banerjee, S. (2020). Bayesian spatially varying coefficient models in the spBayes R package. *Environmental Modelling and Software*, 125.
- Franco-Villoria, M., Ventrucci, M., and Rue, H. (2019). A unified view on Bayesian varying coefficient models. arXiv:1806.02084v2.
- Friedman, J. H. (1991). Multivariate adaptive regression splines. *Annals of Statistics*, 19(1):1 – 67.
- Gelfand, A. E., Kim, H.-J., Sirmans, C., and Banerjee, S. (2003). Spatial modeling with spatially varying coefficient processes. *Journal of the American Statistical Association*, 98(462):387 – 396.
- Ghosal, S. and van der Vaart, A. (2017). *Fundamentals of Nonparametric Bayesian Inference*. Cambridge University Press.
- Gramacy, R. B. and Lee, H. K. H. (2009). Adaptive design and analysis of supercomputer experiments. *Technometrics*, 51(2):130 – 145.
- Greenfield, E. A. and Moorman, S. M. (2019). Childhood socioeconomic status and later life cognition: Evidence from the Wisconsin Longitudinal Study. *Journal of aging and health*, 31(9):1589–1615.
- Greenwell, B., Boehmke, B., Cunningham, J., and GBM Developers (2019). *gbm: Generalized boosted regression models*. R package version 2.1.5.
- Gross, A. L., Mungas, D. M., Crane, P. K., Gibbons, L. E., MacKay-Brandt, A., Manly, J. J., Mukherjee, S., Romero, H., Sachs, B., Thomas, M., et al. (2015). Effects of education and race on cognitive decline: An integrative study of generalizability versus study-specific results. *Psychology and aging*, 30(4):863.

- Guhaniyogi, R., Li, C., Savitsky, T. D., and Srivastava, S. (2020). Distributed Bayesian varying coefficient modeling using a Gaussian process prior. arXiv:2006.007831v1.
- Hahn, P. R., Murray, J. S., and Carvalho, C. M. (2020). Bayesian regression models for causal inference: regularization, confounding, and heterogeneous effects. *Bayesian Analysis*.
- Hastie, T. and Tibshirani, R. (1993). Varying-coefficient models. *Journal of the Royal Statistical Society – Series B (Methodological)*, 55(4):757 – 796.
- Hayfield, T. and Racine, J. S. (2008). Nonparametric econometrics: The np package. *Journal of Statistical Software*, 27(5).
- Hill, J. L. (2011). Bayesian nonparametric modeling for causal inference. *Journal of Computational and Graphical Statistics*, 20(1):217–240.
- Hoover, D. R., Rice, J. A., Wu, C. O., and Yang, L.-P. (1998). Nonparametric smoothing estimates of time-varying coefficient models with longitudinal data. *Biometrika*, 85(4):809 – 822.
- Huang, J. Z., Wu, C. O., and Zhou, L. (2002). Varying-coefficient models and basis function approximations for the analysis of repeated measurements. *Biometrika*, 89(1):111 – 128.
- Jorm, A. F., Rodgers, B., Henderson, A. S., Korten, A. E., Jacomb, P. A., Christensen, H., and Mackinnon, A. (1998). Occupation type as a predictor of cognitive decline and dementia in old age. *Age and Ageing*, 27(4):477–483.
- Lee, K., Lee, Y. K., Park, B. U., and Yang, S. J. (2018). Time-dynamic varying coefficient models for longitudinal data. *Computational Statistics and Data Analysis*, 123:50 – 65.
- Li, Q. and Racine, J. S. (2010). Smooth varying-coefficient estimation and inference for qualitative and quantitative data. *Econometric Theory*, 26(6):1607 – 1637.
- Lichtenberg, P. A., Ross, T., Millis, S. R., and Manning, C. A. (1995). The relationship between depression and cognition in older adults: A cross-validation study. *Journals of Gerontology: Series B*, 50B(P25 - P32).
- Linero, A. R. (2018). Bayesian regression trees for high-dimensional prediction and variable selection. *Journal of the American Statistical Association*, 113(522):626 – 636.
- Linero, A. R., Sinha, D., and Lipsitz, S. R. (2019). Semiparametric mixed-scale models using shared Bayesian forests. arXiv:1809.08521v4.

- Linero, A. R. and Yang, Y. (2018). Bayesian regression tree ensembles that adapt to smoothness and sparsity. *Journal of the Royal Statistical Society – Series B (Methodological)*, 80(5):1087 – 1110.
- Liu, H., Waite, L., and Shen, S. (2016). Diabetes risk and disease management in later life: A national longitudinal study of the role of marital quality. *Journals of Gerontology Series B: Psychological Sciences and Social Sciences*, 71(6):1070–1080.
- Luo, Y. and Waite, L. J. (2005). The impacts of childhood and adult SES on physical, mental, and cognitive well-being in later life. *The Journals of Gerontology: Series B*, 60(2):S93 – S101.
- Lyu, J. and Burr, J. (2016). Socioeconomic status across the life course and cognitive function among older adults: An examination of the latency, pathways, and accumulate hypotheses. *Journal of Aging Health*, 28(1):40 – 67.
- Marden, J., Tchetgen Tchetgen, E. J., Kawachi, I., and Glymour, M. (2017). Contribution of socioeconomic status and 3 life-course periods to late-life memory function and decline: early and late predictors of dementia risk. *American Journal of Epidemiology*, 186(7):805 – 814.
- McCulloch, R., Sparapani, R., Gramacy, R., Spanbauer, C., and Pratola, M. (2018). *BART: Bayesian additive regression trees*. R package version 2.1.
- Murray, J. S. (2019). Log-linear Bayesian additive regression trees for categorical and count response. arXiv:1701.01503v2.
- Piccinin, A. M., Muniz-Terrera, G., Clouston, S., Reynolds, C. A., Thorvaldsson, V., Deary, I. J., Deeg, D. J., Johansson, B., Mackinnon, A., Spiro III, A., et al. (2013). Coordinated analysis of age, sex, and education effects on change in mmse scores. *Journals of Gerontology Series B: Psychological Sciences and Social Sciences*, 68(3):374–390.
- Pratola, M. T. (2016). Efficient Metropolis-Hastings proposal mechanisms for Bayesian regression tree models. *Bayesian Analysis*, 11(3):885 – 911.
- R Core Team (2019). *R: A language and environment for statistical computing*. R Foundation for Statistical Computing, Vienna, Austria.
- Ročková, V. and Saha, E. (2019). On theory for BART. In *Proceedings of Machine Learning Research*, volume 89, pages 2839–2848.

- Ročková, V. and van der Pas, S. (2019). Posterior concentration for Bayesian regression trees and forests. *Annals of Statistics*.
- Seblova, D., Berggren, R., and Lövdén, M. (2020). Education and age-related decline in cognitive performance: Systematic review and meta-analysis of longitudinal cohort studies. *Ageing Research Reviews*, 58:101005.
- Sisco, S., Gross, A. L., Shih, R. A., Sachs, B. C., Glymour, M. M., Bangen, K. J., Benitez, A., Skinner, J., Schneider, B. C., and Manly, J. J. (2015). The role of early-life educational quality and literacy in explaining racial disparities in cognition in late life. *Journals of Gerontology Series B: Psychological Sciences and Social Sciences*, 70(4):557–567.
- Sonnega, A., Faul, J., Ofstedal, M., Langa, K. M., Phillips, J. W., and Weir, D. R. (2014). Cohort profile: The Health and Retirement Study (HRS). *International Journal of Epidemiology*, 43(2):576 – 585.
- Sparapani, R., Logan, B. R., McCulloch, R. E., and Laud, P. W. (2016). Nonparametric survival analysis using Bayesian additive regression trees. *Statistics in Medicine*, 35(16):2741 – 2753.
- Starling, J. E., Aiken, C. E., Murray, J. S., Nakimuli, A., and Scott, J. G. (2019a). Monotone function estimation in the presence of extreme data coarsening: Analysis of preeclampsia and birth weight in urban Uganda. arXiv:1912.06946.
- Starling, J. E., Murray, J. S., Carvalho, C. M., Bukowski, R., and Scott, J. G. (2019b). BART with targeted smoothing: An analysis of patient-specific stillbirth risk. arXiv:1805.07656v7.
- Tan, Y. V. and Roy, J. (2019). Bayesian additive regression trees and the General BART model. arXiv:1901.07504v1.
- Tibshirani, R. and Friedman, J. (2019). A pliable lasso. *Journal of Computational and Graphical Statistics*.
- Vable, A. M., Gilsanz, P., Nguyen, T. T., Kawachi, I., and Glymour, M. M. (2017). Validation of a theoretically motivated approach to measuring childhood socioeconomic circumstances in the Health and Retirement Study. *PLoS ONE*, 12(10):e0185898.
- Wang, H. and Xia, Y. (2009). Shrinkage estimation for the varying coefficient model. *Journal of the American Statistical Association*, 104(486):747 – 757.

- Wang, J. C. and Hastie, T. (2012). Boosted varying-coefficient regression models for product demand prediction. *Journal of Computational and Graphical Statistics*, 23(2):361 – 382.
- Wang, L., Li, H., and Huang, J. Z. (2008). Variable selection in nonparametric varying-coefficient models for analysis of repeated measurements. *Journal of the American Statistical Association*, 103(484):1556 – 1569.
- Wei, F., Huang, J., and Li, H. (2011). Variable selection and estimation in high-dimensional varying-coefficient models. *Statistica Sinica*, 21:1515 – 1540.
- Wilson, R., Hebert, L., Scherr, P., Barnes, L., De Leon, C. M., and Evans, D. (2009). Educational attainment and cognitive decline in old age. *Neurology*, 72(5):460–465.
- Wilson, R. S., Capuano, A. W., Systema, J., Bennett, D. A., and Barnes, L. L. (2015). Cognitive aging in older black and white persons. *Psychology and Aging*, 30(2):279 – 285.
- Woody, S., Carvalho, C. M., Hahn, P. R., and Murray, J. S. (2020). Estimating heterogeneous effects of continuous exposures using Bayesian tree ensembles: Revising the impact of abortion rates on crime. arXiv:2007.09845v1.
- Wright, M. N. and Ziegler, A. (2017). ranger: A fast implementation of random forests for high dimensional data in C++ and R. *Journal of Statistical Software*, 77(1):1 – 17.
- Wu, C. O. and Chiang, C.-T. (2000). Kernel smoothing on varying coefficient models with longitudinal dependent variable. *Statistica Sinica*, 10:433 – 456.
- Xu, D., Daniels, M. J., and Winterstein, A. G. (2016). Sequential BART for imputation of missing covariates. *Biostatistics*, 17(3):589 – 602.
- Zahodne, L. B., Glymour, M. M., Sparks, C., Bontempo, D., Dixon, R. A., MacDonald, S. W., and Manly, J. J. (2011). Education does not slow cognitive decline with aging: 12-year evidence from the victoria longitudinal study. *Journal of the International Neuropsychological Society*, 17(6):1039.
- Zhang, Z., Liu, H., and Choi, S.-w. (2020). Early-life socioeconomic status, adolescent cognitive ability, and cognition in late midlife: Evidence from the Wisconsin Longitudinal Study. *Social Science & Medicine*, 244:112575.
- Zhou, Y. and Hooker, G. (2019). Tree boosted varying coefficient models. arXiv:1904.01058v1.

Supplementary Materials

S1 Gibbs Sampler Details

Recall that we have n_i observations for each subject $i = 1, \dots, n$. We model for each $i = 1, \dots, n$, and $t = 1, \dots, n_i$

$$y_{it} = \beta_0(\mathbf{z}_{it}) + \sum_{j=1}^p \beta_j(\mathbf{z}_{it})x_{itj} + \sigma\varepsilon_{it}, \quad (\text{S1})$$

where $\varepsilon_i \sim \mathcal{N}(\mathbf{0}_{n_i}, \Sigma_i(\rho))$ and the diagonal elements of $\Sigma_i(\rho)$ are equal to one.

Let $\Theta = \{\theta_0, \dots, \theta_p\}$ be the collection of splitting index probabilities. Recall that we model $\theta_j \sim \text{Dirichlet}(\eta_j/R, \dots, \eta_j/R)$ and place a further discretized Beta(1, R) prior over the hyperparameter η_j such that for each $k \in \{0, \dots, 100\}$,

$$\mathbb{P}\left(\frac{\eta_j}{\eta_j + R} = \frac{k}{100}\right) \propto \left(\frac{100 - k}{100}\right)^{R-1}$$

For each subject i , let $\mathbf{R}_i = (R_{i1}, \dots, R_{in_i})^\top$ be the vector of *full residuals* for subject i where

$$R_{it} = y_{it} - \sum_{m=1}^M g(\mathbf{z}_{it}; T_m^{(0)}, \boldsymbol{\mu}_m^{(0)}) - \sum_{j=1}^p \sum_{m=1}^M x_{itj} g(\mathbf{z}_i; T_m^{(j)}, \boldsymbol{\mu}_m^{(j)}).$$

Conditionally on ρ , the joint posterior density of $(\boldsymbol{\mathcal{E}}, \sigma^2, \Theta, \boldsymbol{\eta})$ is given by

$$\begin{aligned} \pi(\boldsymbol{\mathcal{E}}, \sigma^2, \Theta, \boldsymbol{\eta} \mid \mathbf{Y}) &\propto (\nu + \sigma^2)^{-\frac{\nu+1}{2}} \times \prod_{i=1}^n \sigma^{-n_i} |\boldsymbol{\Omega}_i(\rho)|^{\frac{1}{2}} \exp\left\{-\frac{\mathbf{R}_i^\top \boldsymbol{\Omega}_i(\rho) \mathbf{R}_i}{2\sigma^2}\right\} \\ &\times \prod_{j=0}^p \pi(\eta_j) \pi(\boldsymbol{\theta}_j \mid \eta_j) \prod_{m=1}^M \pi(T_m^{(j)} \mid \boldsymbol{\theta}_j) \tau_j^{-L_m^{(j)}} \exp\left\{-\frac{\|\boldsymbol{\mu}_m^{(j)}\|_2^2}{2\tau_j^2}\right\}, \end{aligned} \quad (\text{S2})$$

where $\boldsymbol{\Omega}_i(\rho) = \Sigma_i^{-1}(\rho)$.

We use a Metropolis-Hastings – within – Gibbs sampler to simulate posterior draws of $(\boldsymbol{\mathcal{E}}, \sigma^2, \Theta, \boldsymbol{\eta}) \mid \mathbf{Y}$.

Updating a single tree. We now describe the update of the m^{th} regression tree $(T_m^{(j)}, \boldsymbol{\mu}_m^{(j)})$

in the ensemble \mathcal{E}_j used to approximate β_j . Let \mathcal{E}^- denote the collection of all remaining $M(p+1) - 1$ regression trees, where, for notational compactness, we have suppressed the dependence of this collection on the indices j and m . Additionally, let $\mathbf{r}_i = (r_{i1}, \dots, r_{in_i})^\top$ be the vector of subject i 's *partial residuals* where

$$r_{it} = R_{it} + x_{itj}g(\mathbf{z}_{it}; T_m^{(j)}, \boldsymbol{\mu}_m^{(j)}),$$

where we have again suppressed the dependence of r_{it} on j and m for brevity.

Before describing the update of the tree, we require some additional notation. For an arbitrary decision tree T with L leaves, let $I_i(\ell)$ be the set of indices t such that \mathbf{z}_{it} is contained in leaf ℓ of tree t . That is, $I_i(\ell) = \{t : \ell(\mathbf{z}_{it}) = \ell\}$. Further, let $\mathbf{X}_i(T)$ be the $n_i \times L$ matrix whose (t, ℓ) entry is equal to x_{itj} if $t \in I_i(\ell, T)$ and is zero otherwise. With this additional notation, we have $\mathbf{r}_i = \mathbf{R}_i + \mathbf{X}_i(T_m^{(j)})\boldsymbol{\mu}_m^{(j)}$.

The conditional posterior density of a single regression tree $(T, \boldsymbol{\mu})$ is given by

$$\pi(T, \boldsymbol{\mu} \mid \mathbf{y}, \mathcal{E}^-, \boldsymbol{\Theta}, \boldsymbol{\eta}, \sigma, \rho) \propto \pi(T \mid \boldsymbol{\theta}_j) \tau^{-L(T)} \exp \left\{ -\frac{1}{2} [\boldsymbol{\mu}^\top \Lambda(T)^{-1} \boldsymbol{\mu} - 2\boldsymbol{\mu}^\top \Theta(T)] \right\} \quad (\text{S3})$$

where

$$\begin{aligned} \Lambda(T) &= \left[\tau^{-2} \mathbf{I}_{L(T)} + \sum_{i=1}^n \mathbf{X}_i(T)^\top \boldsymbol{\Omega}_i(\rho) \mathbf{X}_i(T) \right]^{-1} \\ \Theta(T) &= \sum_{i=1}^n \mathbf{X}_i(T)^\top \boldsymbol{\Omega}_i(\rho) \mathbf{r}_i. \end{aligned}$$

In order to update the tree $(T_m^{(j)}, \boldsymbol{\mu}_m^{(j)})$, we use the same strategy as [Chipman et al. \(2010\)](#): we first draw a new decision tree from the marginal distribution $\pi(T \mid \mathbf{Y}, \mathcal{E}^-, \sigma, \boldsymbol{\Theta}, \boldsymbol{\eta}, \sigma)$ with a MH step and then draw a new set of jump conditionally on the new decision tree. To this end, by integrating $\boldsymbol{\mu}$ out of (S3), the marginal posterior mass function of T is given by

$$\pi(T \mid \mathbf{Y}, \mathcal{E}^-, \boldsymbol{\Theta}, \boldsymbol{\eta}, \sigma, \rho) \propto |\Lambda(T)|^{\frac{1}{2}} \tau^{-L(T)} \exp \left\{ \frac{1}{2} \Theta(T)^\top \Lambda(T) \Theta(T) \right\}. \quad (\text{S4})$$

In our MH step, we propose a new tree \tilde{T} by growing or pruning the current tree $T_m^{(j)}$.

We can also read off the conditional density of $\boldsymbol{\mu} \mid T$ directly from (S3)

$$\pi(\boldsymbol{\mu} \mid T, \mathbf{Y}, \boldsymbol{\mathcal{E}}^-, \boldsymbol{\Theta}, \boldsymbol{\eta}, \sigma, \rho) \propto \exp \left\{ -\frac{1}{2} [\boldsymbol{\mu}^\top \Lambda^{-1}(T) \boldsymbol{\mu} - 2\boldsymbol{\mu}^\top \Theta(T)] \right\}, \quad (\text{S5})$$

which is proportional to the density of a $\mathcal{N}(\Lambda(T)\Theta(T), \Lambda(T))$ distribution.

Updating σ . We use another Metropolis-Hastings step to draw a new value of σ from its conditional distribution with density

$$\pi(\sigma \mid \mathbf{Y}, \boldsymbol{\mathcal{E}}, \boldsymbol{\Theta}, \boldsymbol{\eta}, \rho) \propto (\nu + \sigma^2)^{-\frac{\nu+1}{2}} \sigma^{-N} \exp \left\{ -\frac{1}{2\sigma^2} \sum_{i=1}^n \mathbf{R}_i^\top \boldsymbol{\Omega}_i(\rho) \mathbf{R}_i \right\}.$$

In our MH step, we draw a new proposal from a transition kernel Q with density

$$q(\sigma) \propto \sigma^{-3-N} \exp \left\{ -\frac{1}{2\sigma^2} \sum_{i=1}^n \mathbf{R}_i^\top \boldsymbol{\Omega}_i(\rho) \mathbf{R}_i \right\}.$$

Note that if $\sigma \sim Q$, then

$$\sigma^2 \sim \text{Inverse Gamma} \left(\frac{N}{2}, \frac{1}{2} \sum_{i=1}^n \mathbf{R}_i^\top \boldsymbol{\Omega}_i(\rho) \mathbf{R}_i \right).$$

The transition kernel Q is precisely equal to the conditional posterior distribution of σ that we would have obtained had we placed a non-informative Jeffrey's prior on σ^2 with improper density σ^{-2} .

Using the transition kernel Q , which to the best of our knowledge was first suggested by [Linero and Yang \(2018\)](#), facilitates considerable cancellation in the MH acceptance probability. Indeed, if we draw a new proposal $\tilde{\sigma} \sim Q$, then we accept the transition from $\sigma \rightarrow \tilde{\sigma}$ with probability

$$\alpha(\sigma \rightarrow \tilde{\sigma}) = \left(\frac{\nu + \tilde{\sigma}^2}{\nu + \sigma^2} \right)^{-\frac{1+\nu}{2}} \times \left(\frac{\tilde{\sigma}}{\sigma} \right)^3.$$

Updating $\boldsymbol{\theta}_j$ and η_j . When we update each decision tree $T_m^{(j)}$ in the ensemble \mathcal{E}_j , we track the number of times that each modifier is used in This facilitates a simple Dirichlet-Multinomial conjugate update for $\boldsymbol{\theta}_j$. Since the prior on η_j , is discrete, it is straightforward to sample directly from the conditional posterior $\pi(\eta_j \mid \mathcal{E}_j, \boldsymbol{\theta}_j, \mathbf{Y})$. For further details, see [Linero \(2018\)](#).

Computational complexity. Each regression tree update involves computing a sum of the form

$$\sum_{i=1}^n \mathbf{X}_i(T)^\top \boldsymbol{\Omega}_i(\rho) \mathbf{X}_i(T).$$

For a general tree with L leaves and a general $\boldsymbol{\Omega}_i(\rho)$, computing this sum requires $O(L^2 \sum_{i=1}^n n_i^2)$. Thanks to the strong regularization imposed by [Chipman et al. \(2010\)](#)'s branching process prior, however, the number of leaves L is usually quite small relative to n . As a result, the complexity of a single tree update for a general error correlation structure is essentially $O(\sum_{i=1}^n n_i^2)$. Similarly, to update σ , we must compute $\sum_{i=1}^n \mathbf{R}_i^\top \boldsymbol{\Omega}_i(\rho) \mathbf{X}_i(T)$, which has the same complexity. However, if we assume a compound symmetry error correlation structure, in which all off-diagonal elements of $\boldsymbol{\Sigma}_i(\rho)$ are equal to ρ , we can compute this quadratic form with $O(n_i)$ operations, resulting in a per-iteration complexity of $O(NMp)$.

The complexity of updating $\boldsymbol{\theta}_j$ and η_j is $O(R)$, which is negligible when N is substantially larger than R .

S2 Hyperparameter Sensitivity

Recall from the main text, that each ensemble \mathcal{E}_j contained $M = 50$ trees and we set the prior jump variance $\tau_j = M^{-\frac{1}{2}}$. This induced a marginal $\mathcal{N}(0, 1)$ prior on each evaluation $\beta_j(\mathbf{z})$. Of course, if one has strong prior beliefs about the range of covariate effects, one can set τ_j in such a way that the implied marginal prior on $\beta_j(\mathbf{z})$ places substantial probability on this range. In this section, we consider the sensitivity of VCBART's covariance effect recovery and predictive capabilities to different choices of τ_j . Specifically, we replicate the synthetic data experiment from Section 4 of the main text keeping $M = 50$ fixed but setting each $\tau_j = \tau M^{-\frac{1}{2}}$ with $\tau \in \{0.25, 0.5, 1, 2, 4\}$.

Figure S1 is the analog of Figure 2 in the main text, comparing the covariate effect recovery and predictive performance of VCBART with different values of τ_j . Uncertainty interval and predictive interval lengths are reported relative to our recommended setting $\tau = 1$; values greater than one indicate that a particular setting of τ results in less posterior uncertainty than $\tau = 1$.

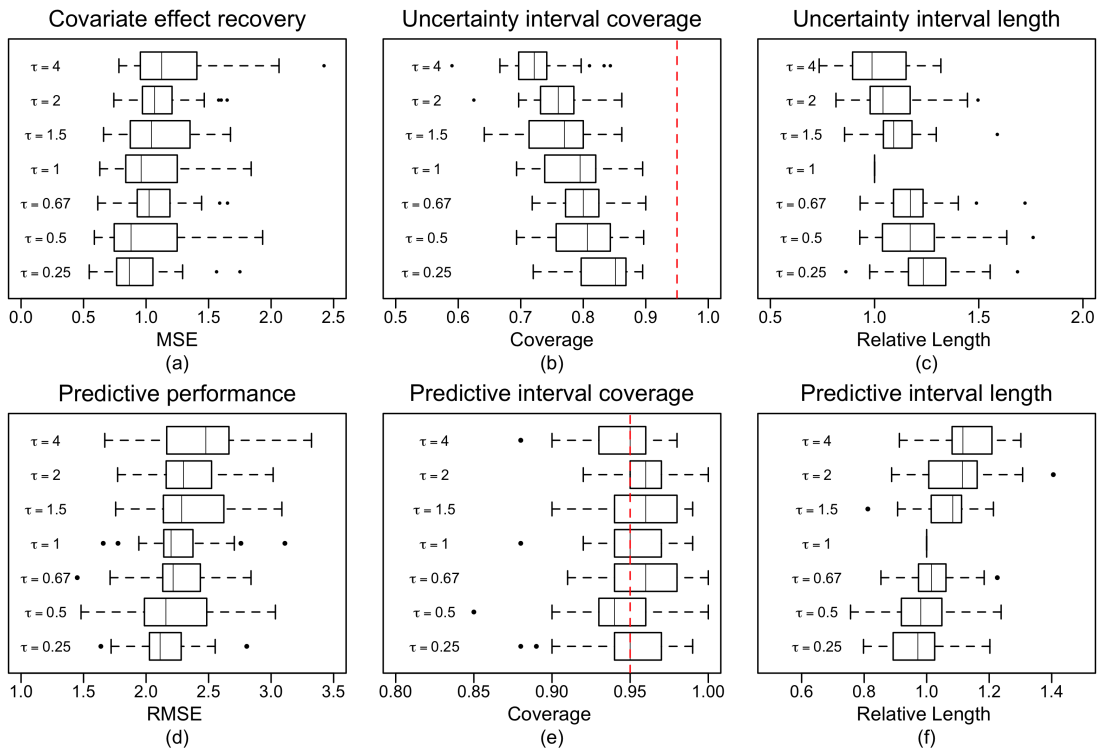


Figure S1: (a) Total mean square error for estimating β_j . (b) Frequentist coverage of 95% uncertainty intervals for $\beta_j(\mathbf{z})$. (c) Lengths of 95% uncertainty intervals relative to VCBART with $\tau = 1$. (d) Out-of-sample predictive root mean square error. (e) Coverage of 95% prediction intervals. (f) Lengths of 95% prediction intervals relative to VCBART with $\tau = 1$. All performance measures reported over 25 training–testing splits.

In Figures S1(a) and (d), we find that as we introduce less shrinkage (i.e. increase τ), the overall MSE for estimating the β_j 's and the out-of-sample predictive RMSE tends to increase. We further see in Figures S1(b) and (c) that increasing τ produced somewhat shorter uncertainty intervals about the estimated $\beta_j(\mathbf{z})$ with decreasing frequentist coverage. Interestingly, when we look at the predictive intervals, we find that the overall coverage is relatively insensitive to increasing τ (Figure S1(e)) but the predictive intervals get longer (Figure S1(f)). Although VCBART is somewhat sensitive to the choice of τ_j , none of the values of τ that we considered led to performance that was worse than any of KS, TVCM, or BTVM.

S3 Simulation Details and Additional Results

S3.1 Implementation and experimental details

VCBART is implemented in C++ and interfaces with R (R Core Team, 2019) through Rcpp (Eddelbuettel and François, 2011) and RcppArmadillo Eddelbuettel and Sanderson (2014). Our implementation uses the basic class structures of tsBART (Starling et al., 2019b). We have created an R package **VCBART**, which is included in the supplemental materials. We performed all of the experiments reported in Sections 4 and 5 of the main text on a high performance computing cluster. All of the experiments were run in R version 3.6.2 on nodes with 8 GB of RAM and running an Intel Xeon Gold 6248 processor.

Where possible, we ran the competing methods in our simulations with package defaults and did not implement any additional tuning procedures. For instance, the default implementation of Zhou and Hooker (2019)’s boosted tree procedure (referred to as BTVCN in Sections 4 and 5 of the main text) does not automatically perform cross-validation to set the learning rate or number of boosting iterations. Instead, in all of our experiments, we ran BTVCN for 200 iterations and with a learning rate of 0.5, which are the same settings as the example provided by the authors at <https://github.com/siriuz42/treeboostVCM>. Similarly the implementation of extremely randomized trees in the **ranger** package (Wright and Ziegler, 2017) does not automatically perform cross-validation to select the number of possible splitting variables at each node (i.e. the parameter `mtry`). In our experiments, we used the package default, setting `mtry` equal to the square root of the number of inputs.

S3.2 Function-by-function covariate recovery performance

In the main text, we reported the covariate effect function recovery performance averaged over all β_j ’s. Across the 25 training–testing splits considered in Section 4 of the main text, VCBART produced consistently more accurate estimates of each individual function β_j (Figure S2). Figures S3 and S4 compare the frequentist coverage and relative lengths of the 95% uncertainty intervals for each function. For each function, VCBART’s 95% credible intervals tended to be narrower than the bootstrapped confidence intervals for KS, TVCM, and BTVCN. However, the frequentist coverage of VCBART’s 95% credible intervals tended to be closer to 85% for each function, with the exception of β_3 , which was the constant zero function.

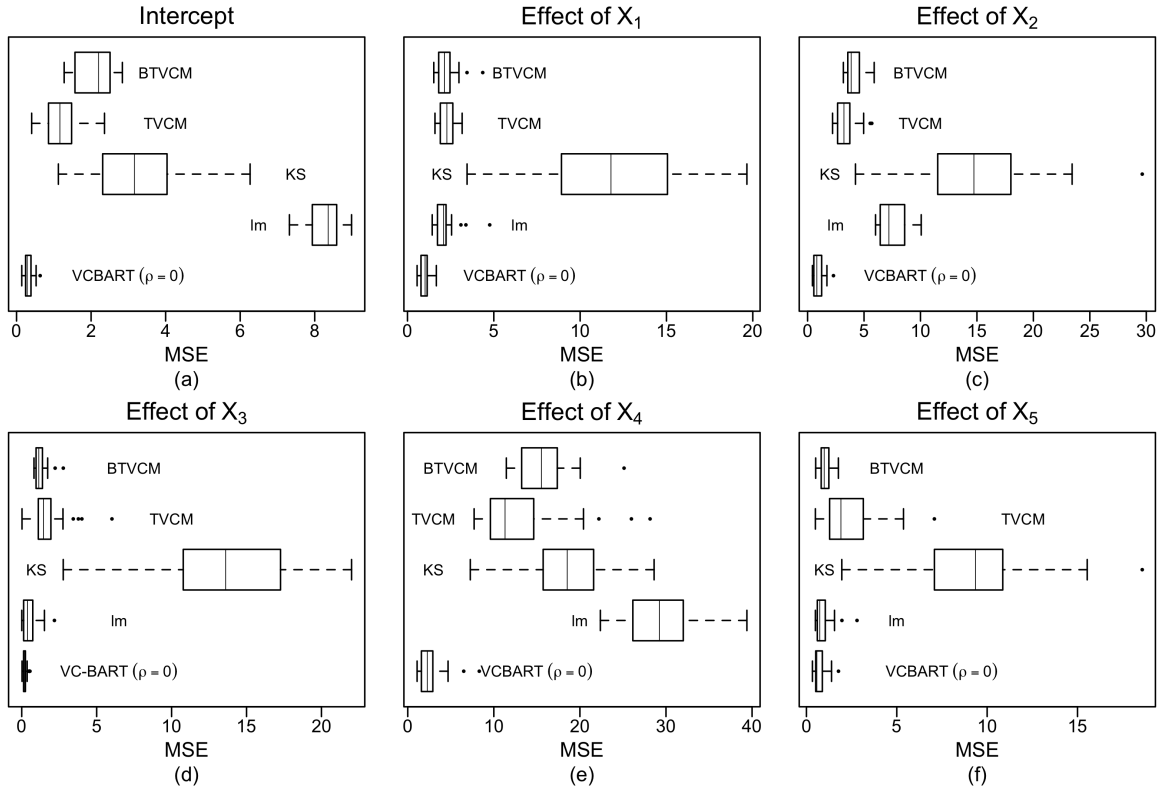


Figure S2: Mean square error for estimating each β_j .

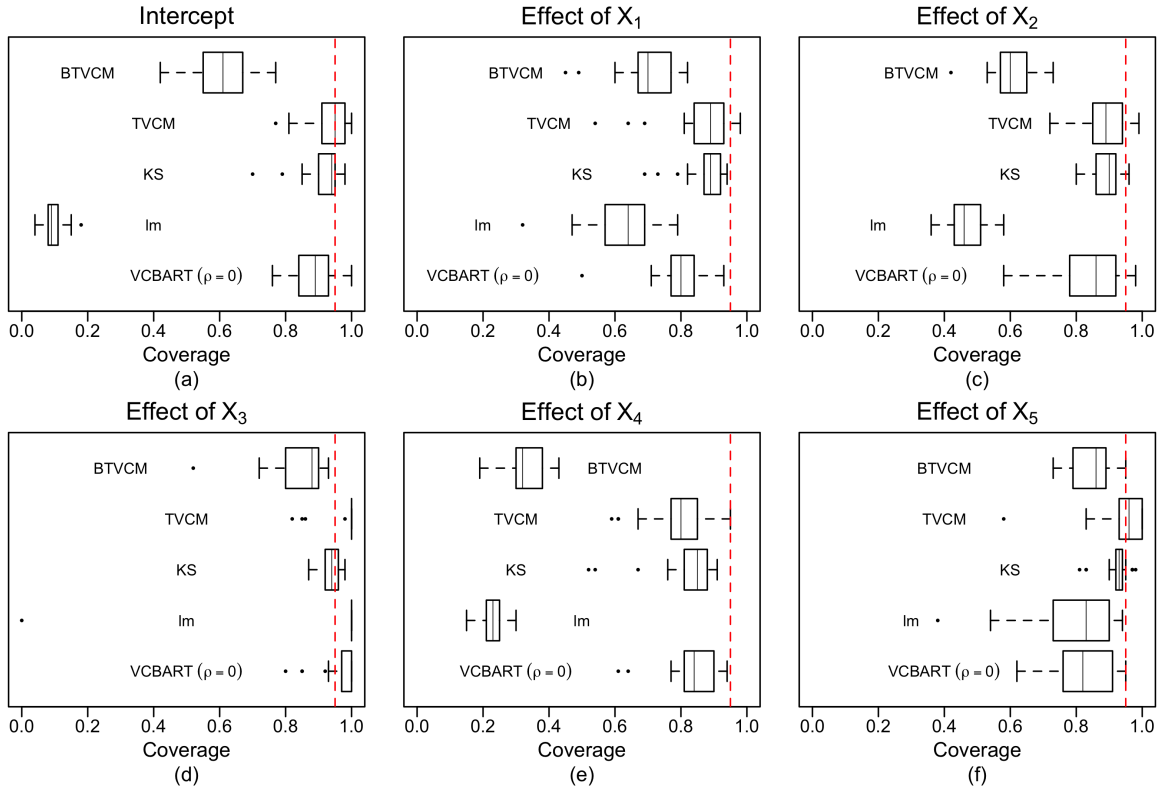


Figure S3: Frequentist coverage of the 95% uncertainty intervals for each β_j .

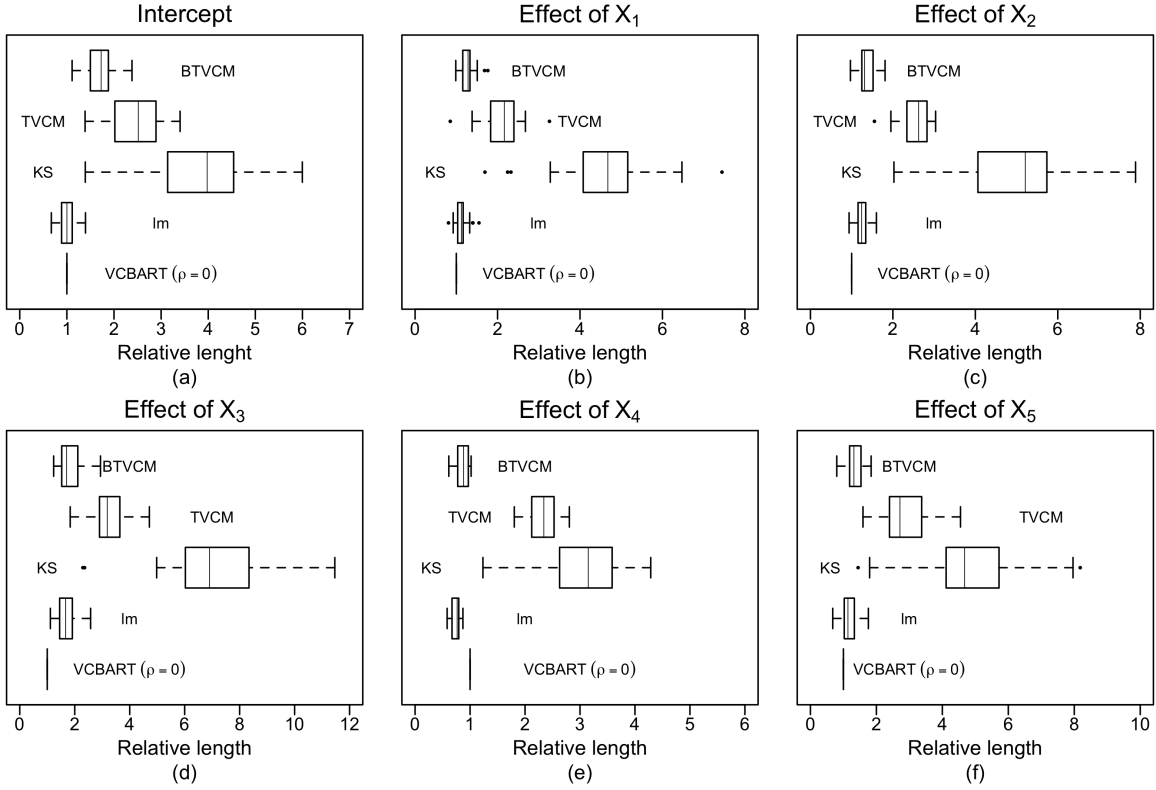


Figure S4: Lengths of the 95% uncertainty intervals for each β_j relative to VCBART with $\rho = 0$.

S4 Proofs for Asymptotic Results

S4.1 Notation and Preliminaries

The proof of Theorem 1 is based on the standard prior concentration and testing arguments outlined in Ghosal and van der Vaart (2017). Roughly speaking, in order to prove optimal posterior concentration, the prior on $\boldsymbol{\beta} = [\beta_0, \dots, \beta_p]$ first needs to be “close” enough to $\boldsymbol{\beta}_0$ (i.e. the prior needs to assign enough positive probability mass to a neighborhood of $\boldsymbol{\beta}_0$). Second, we need to construct exponentially powerful statistical tests, so that the probabilities of Type I and Type II errors for testing $H_0 : \boldsymbol{\beta} = \boldsymbol{\beta}_0$ vs. $H_1 : \{\|\boldsymbol{\beta} - \boldsymbol{\beta}_0\|_n > r_n\}$ are exponentially decreasing.

Throughout this section, we use the following notation. For two nonnegative sequences $\{a_n\}$ and $\{b_n\}$, we write $a_n \asymp b_n$ to denote $0 < \liminf_{n \rightarrow \infty} a_n/b_n \leq \limsup_{n \rightarrow \infty} a_n/b_n < \infty$. If $\lim_{n \rightarrow \infty} a_n/b_n = 0$, we write $a_n = o(b_n)$ or $a_n \prec b_n$. We use $a_n \lesssim b_n$ or $a_n = O(b_n)$ to denote that for sufficiently large n , there exists a constant $C > 0$ independent of n such that $a_n \leq Cb_n$. For a function β , $\|\beta\|_\infty = \max_{\mathbf{z} \in [0,1]^R} |\beta(\mathbf{z})|$. Finally, for a symmetric matrix \mathbf{A} , we let $\lambda_{\min}(\mathbf{A})$ and $\lambda_{\max}(\mathbf{A})$ denote its minimum and maximum eigenvalues

For two densities f and g , let $K(f, g) = \int f \log(f/g)$ and $V(f, g) = \int f |\log(f/g) - K(f/g)|^2$ denote the Kullback-Leibler (KL) divergence and KL variation respectively. Denote the Rényi divergence of order $1/2$ as $\rho(f, g) = -\log \int f^{1/2} g^{1/2} d\nu$. Finally, denote the ε -covering number for a set Ω with semimetric d as the minimum number of d -balls of radius ε needed to cover Ω and denote the ε -covering number as $N(\varepsilon, \Omega, d)$ and the metric entropy as $\log N(\varepsilon, \Omega, d)$.

To prove near-optimal posterior concentration for VCBART, we need to make the following assumptions. Below, we let $\alpha_{\min} := \min\{\alpha_0, \dots, \alpha_p\}$ and $n_{\max} = \max\{n_1, \dots, n_n\}$.

(A1) $\|\beta_{0,j}\|_\infty < \infty$ for $0 \leq j \leq p$.

(A2) There exists a constant $D > 0$ so that $|x_{itj}| \leq D$ for all $1 \leq i \leq n, 1 \leq t \leq n_i, 1 \leq j \leq p$.

(A3) $p = o(N^{2\alpha_{\min}/(2\alpha_{\min}+R)}/\log N)$, $R = O((\log N)^{1/2})$, and $n_{\max} \asymp N/n$.

(A4) The eigenvalues of each within-subject correlation matrix $\boldsymbol{\Sigma}_i$ satisfy

$$1 \lesssim \min_{1 \leq i \leq n} \lambda_{\min}(\boldsymbol{\Sigma}_i(\rho_0)) \leq \max_{1 \leq i \leq n} \lambda_{\max}(\boldsymbol{\Sigma}_i(\rho_0)) \lesssim 1,$$

and for any $(\sigma_1^2, \rho_1), (\sigma_2^2, \rho_2) \in (0, \infty) \times (0, 1)$

$$\begin{aligned} \max_{1 \leq i \leq n} \|\sigma_1^2 \boldsymbol{\Sigma}_i(\rho_1) - \sigma_2^2 \boldsymbol{\Sigma}_i(\rho_2)\|_F^2 &\leq \frac{1}{n} \|\sigma_1^2 \boldsymbol{\Sigma}(\rho_1) - \sigma_2^2 \boldsymbol{\Sigma}(\rho_2)\|_F^2 \\ &\lesssim n_{\max}^2 (\sigma_1^2 - \sigma_2^2)^2 + n_{\max}^4 \sigma_2^2 |\rho_1 - \rho_2|^2. \end{aligned}$$

where $\boldsymbol{\Sigma} = \text{diag}(\boldsymbol{\Sigma}_1, \dots, \boldsymbol{\Sigma}_n)$.

Assumption (A1) requires the true $\beta_{0,j}$'s to be uniformly bounded. Since the effect modifiers \mathbf{z} have been rescaled to lie in $[0, 1]^R$, this assumption is likely to be satisfied in practice. Assumption (A2) requires that the covariates x_{itj} are uniformly bounded for all i, t, j . Assumption (A3) allows the number of covariates p to diverge to infinity but at a slower rate than N . This assumption is needed to ensure that the contraction rate converges to zero as $n, p \rightarrow \infty$. Assumption (A3) also allows the number of effect modifiers R to grow with n , but at a much slower rate. Assumption (A4) assumes that the within-subject correlation matrices are asymptotically well-behaved in the sense that the eigenvalues for every $\boldsymbol{\Sigma}_i$ are bounded away from zero and infinity, and the maximum squared Frobenius norm for the difference between any two correlation matrices of size $n_i \times n_i$ is bounded above by a function of n_{\max} . Many commonly used correlation structures like first-order autoregressive, compound symmetry, and moving average satisfy this assumption.

S4.2 Proof of Theorem 1

Let $\theta_{it} = \sum_{j=0}^p \beta_{0,j}(\mathbf{z}_{it}) x_{itj}$, and let $\boldsymbol{\theta}_i = (\theta_{i1}, \dots, \theta_{in_i})^\top$ denote the $n_i \times 1$ vector corresponding to the i th subject. Let $\boldsymbol{\theta} = (\boldsymbol{\theta}_1^\top, \dots, \boldsymbol{\theta}_n^\top)^\top$ be the $N \times 1$ vector of all the $\boldsymbol{\theta}_i$'s. Let $\theta_{0,it} = \sum_{j=0}^p \beta_{0,j}(\mathbf{z}_{it}) x_{itj}$ and define $\boldsymbol{\theta}_{0,i} = (\theta_{0,i1}, \dots, \theta_{0,in_i})^\top$ and $\boldsymbol{\theta}_0 = (\boldsymbol{\theta}_{0,1}^\top, \dots, \boldsymbol{\theta}_{0,n}^\top)^\top$. Let $\mathbb{P}_{\beta_0}^{(N)}$ denote the probability measure underlying the true model,

$$y_{it} = \beta_{0,0}(\mathbf{z}_{it}) + \sum_{j=0}^p \beta_{0,j}(\mathbf{z}_{it}) x_{itj} + \sigma_0 \varepsilon_{it}, \quad 1 \leq i \leq n, 1 \leq t \leq n_i, \quad (\text{S6})$$

where $\boldsymbol{\varepsilon}_i = (\varepsilon_{i1}, \dots, \varepsilon_{in_i})' \stackrel{\text{ind}}{\sim} \mathcal{N}_{n_i}(\mathbf{0}_{n_i}, \boldsymbol{\Sigma}_i(\rho_0)), \rho_0 \in [0, 1)$. Recall that $N = \sum_{i=1}^n n_i$ is the total number of observations. For the i th observation, the response $\mathbf{y}_i = (y_{i1}, \dots, y_{in_i})^\top$ is distributed as $\mathbf{y}_i \sim \mathcal{N}_{n_i}(\boldsymbol{\theta}_i, \sigma^2 \boldsymbol{\Sigma}_i(\rho_0))$. Let f_i denote the density for \mathbf{y}_i and $f = \prod_{i=1}^n f_i$. Analogously, let $f_{0,i}$ be the density for $\mathbf{y}_i \sim \mathcal{N}_{n_i}(\boldsymbol{\theta}_{0,i}, \sigma^2 \boldsymbol{\Sigma}_i(\rho_0))$, and let $f_0 = \prod_{i=1}^n f_{0,i}$.

The proof of Theorem 1 can be sketched as follows. First we establish the optimal *prior*

concentration for the VCBART prior in Lemma 2 and the optimal posterior contraction with respect to average Rényi divergence of order 1/2 in Lemma 3. This will then imply the optimal posterior contraction in the empirical ℓ_2 norm.

Lemma 2. *Under (S6), suppose we endow $(\boldsymbol{\beta}, \sigma)$ with the VCBART prior and the autoregressive parameter ρ with the uniform prior, $\rho \sim \mathcal{U}(0, 1)$. For the BART priors on the β_j 's, $j = 0, \dots, p$, suppose that the splitting probability of a node is $q(d) = \gamma^d$ for some $1/N \leq \gamma < 1/2$ and that the splitting indices are chosen uniformly (i.e. $\boldsymbol{\theta} = (1/R, \dots, 1/R)$). For the half- t_ν prior on σ , assume $\nu > 1$. Assume that Assumptions (A1)-(A4) hold. Then for $r_N^2 = \log N \sum_{j=0}^p N^{-2\alpha_j/(2\alpha_j+R)}$ and some $C_1 > 0$,*

$$\Pi(K(f_0, f) \leq nr_N^2, V(f_0, f) \leq Nr_N^2) \gtrsim \exp(-C_1 Nr_N^2). \quad (\text{S7})$$

Proof of Lemma 2. Our proof follows along the same lines as the proof of Lemma 1 in Bai et al. (2019), with suitable modifications for the fact that we use BART priors on the functionals $\boldsymbol{\beta}$. Denote $\boldsymbol{\Sigma}_i^* = (\sigma^2/\sigma_0^2)\boldsymbol{\Sigma}_{0i}^{-1/2}\boldsymbol{\Sigma}_i\boldsymbol{\Sigma}_{0i}^{-1/2}$, $i = 1, \dots, n$. Denote the ordered eigenvalues of $\boldsymbol{\Sigma}_i^*$ by λ_{it} , $1 \leq t \leq n_i$, and let $\boldsymbol{\Sigma}^* = \text{diag}(\boldsymbol{\Sigma}_1^*, \dots, \boldsymbol{\Sigma}_n^*)$. Noting that the n subjects are independent, we have

$$\begin{aligned} K(f_0, f) &= \frac{1}{2} \left\{ \sum_{i=1}^n \sum_{t=1}^{n_i} (\lambda_{it} - 1 - \log \lambda_{it}) + \frac{\|\boldsymbol{\Sigma}^{-1/2}(\boldsymbol{\theta} - \boldsymbol{\theta}_0)\|_2^2}{\sigma^2} \right\}, \\ V(f_0, f) &= \left[\sum_{i=1}^n \sum_{t=1}^{n_i} \frac{(1 - \lambda_{it})^2}{2} \right] + \frac{\sigma_0^2}{(\sigma^2)^2} \|\boldsymbol{\Sigma}_0^{1/2}\boldsymbol{\Sigma}^{-1}(\boldsymbol{\theta} - \boldsymbol{\theta}_0)\|_2^2. \end{aligned}$$

Define the sets,

$$\begin{aligned} \mathcal{A}_1 &= \left\{ \sigma : \sum_{i=1}^n \sum_{t=1}^{n_i} (\lambda_{ij} - 1 - \log \lambda_{ij}) \leq Nr_N^2, \sum_{i=1}^n \sum_{t=1}^{n_i} (1 - \lambda_{ij})^2 \right\}, \\ \mathcal{A}_2 &= \left\{ (\boldsymbol{\beta}, \sigma) : \frac{\|\boldsymbol{\Sigma}^{-1/2}(\boldsymbol{\theta} - \boldsymbol{\theta}_0)\|_2^2}{\sigma^2} \leq Nr_N^2, \frac{\sigma_0^2}{(\sigma^2)^2} \|\boldsymbol{\Sigma}_0^{1/2}\boldsymbol{\Sigma}^{-1}(\boldsymbol{\theta} - \boldsymbol{\theta}_0)\|_2^2 \leq \frac{Nr_N^2}{2} \right\}. \end{aligned}$$

Then $\Pi(K(f_0, f) \leq Nr_N^2, V(f_0, f) \leq Nr_N^2) = \Pi(\mathcal{A}_2|\mathcal{A}_1)\Pi(\mathcal{A}_1)$, and so we can consider $\Pi(\mathcal{A}_2|\mathcal{A}_1)$ separately. Using almost identical arguments as those in the proof of Lemma 1 of Bai et al. (2019),

$$\Pi(\mathcal{A}_1) \gtrsim \exp(-C_1 Nr_N^2/2), \quad (\text{S8})$$

for some $C_1 > 0$. Next we focus on bounding $\Pi(\mathcal{A}_2|\mathcal{A}_1)$ from below. Similarly as in the

proof of Lemma 1 of Bai et al. (2019), the left-hand side for both inequalities in the set \mathcal{A}_2 , conditional on \mathcal{A}_1 , can be bounded above by a constant multiple of $\|\boldsymbol{\theta} - \boldsymbol{\theta}_0\|_2^2$. Thus, for some constant $b_1 > 0$, we have as a lower bound for $\Pi(\mathcal{A}_2|\mathcal{A}_1)$,

$$\begin{aligned}
\Pi(\mathcal{A}_2|\mathcal{A}_1) &\geq \Pi\left(\boldsymbol{\beta} : \|\boldsymbol{\theta} - \boldsymbol{\theta}_0\|_2^2 \leq \frac{Nr_N^2}{2b_1}\right) \\
&= \Pi\left(\boldsymbol{\beta} : \sum_{i=1}^n \sum_{t=1}^{n_i} \left[\sum_{j=0}^p \beta_j(\mathbf{z}_{it})x_{ij} - \sum_{j=0}^p \beta_{0,j}(\mathbf{z}_{it})x_{ij} \right]^2 \leq \frac{Nr_N^2}{2b_1}\right) \\
&\geq \Pi\left(\boldsymbol{\beta} : \sum_{i=1}^n \sum_{t=1}^{n_i} \sum_{j=0}^p [\beta_j(\mathbf{z}_{it}) - \beta_{0,j}(\mathbf{z}_{it})]^2 \leq \frac{Nr_N^2}{2b_1 D^2(p+1)}\right) \\
&\geq \prod_{j=0}^p \Pi\left(\beta_j : \sum_{i=1}^n \sum_{t=1}^{n_i} [\beta_j(\mathbf{z}_{it}) - \beta_{0,j}(\mathbf{z}_{it})]^2 \leq \frac{N(r_N^j)^2}{2b_1 D^2(p+1)}\right) \\
&\geq \prod_{j=0}^p \Pi\left(\beta_j : \|\beta_j - \beta_{0,j}\|_N \leq \frac{r_N^j}{D_2 \sqrt{2b_1(p+1)}}\right), \tag{S9}
\end{aligned}$$

where $r_N^j = N^{-\alpha_j/(2\alpha_j+R)} \log^{1/2} N$, $j = 0, \dots, p$, and we used Assumption (A2) about the uniform boundedness of the covariates and an application of the Cauchy-Schwarz inequality in the third line of the display. Since we want to show that $\Pi(\mathcal{A}_2|\mathcal{A}_1) \gtrsim \exp(-C_1 Nr_N^2/2)$, it suffices to show (based on the last line of (S9)) that for each function β_j , $j = 0, \dots, p$,

$$\Pi\left(\beta_j : \|\beta_j - \beta_{0,j}\|_N \leq \frac{r_N^j}{D_2 \sqrt{2b_1(p+1)}}\right) \gtrsim e^{-C_1 N(r_N^j)^2/2}. \tag{S10}$$

Note that the lower bound in (S10) holds due to Assumption (A1) that $\|\beta_{0,j}\|_\infty \prec \log^{1/2} N$ for all $1 \leq j \leq p$, Assumption (A3) that $R = O((\log N)^{1/2})$, and the proof of Theorem 7.1 of Ročková and Saha (2019). Thus, from (S9)-(S10), we have that $\Pi(\mathcal{A}_2|\mathcal{A}_1)$ is lower bounded by $\exp(-C_1 Nr_N^2)$. Combined with (S8), this yields the desired lower bound in (S7). \square

Next, we prove posterior contraction of f to the truth f_0 with respect to average Rényi divergence of order $1/2$.

Lemma 3. *Under (S6), suppose we endow $(\boldsymbol{\beta}, \sigma)$ with the VCBART prior and the autoregressive parameter ρ with the uniform prior, $\rho \sim \mathcal{U}(0, 1)$. For the BART priors on the β_j 's, $j = 0, \dots, p$, suppose that the splitting probability of a node is $q(d) = \gamma^d$ for some $1/N \leq \gamma < 1/2$ and that the splitting indices are chosen uniformly (i.e. $\boldsymbol{\theta} = (1/R, \dots, 1/R)$).*

For the half- t_ν prior on σ , assume $\nu > 1$. Assume that Assumptions (A1)-(A4) hold. Then for $r_N^2 = \log N \sum_{j=0}^p N^{-2\alpha_j/(2\alpha_j+R)}$ and some $C_2 > 0$,

$$\Pi \left(\frac{1}{N} \rho(f, f_0) \geq C_2 r_N^2 | \mathbf{Y} \right) \rightarrow 0, \quad (\text{S11})$$

in $\mathbb{P}_{f_0}^{(N)}$ probability as $N, p \rightarrow \infty$.

Proof of Lemma 3. This statement will be proven if we can establish that for some $C_1, C_3 > 0$,

$$\Pi \left(K(f_0, f) \leq N r_N^2, V(f_0, f) \leq N r_N^2 \right) \gtrsim \exp(-C_1 N r_N^2), \quad (\text{S12})$$

as well as the existence of a sieve $\{\mathcal{F}_N\}_{N=1}^\infty$ such that

$$\Pi(\mathcal{F}_N^c) \leq \exp(-C_3 N r_N^2), \quad (\text{S13})$$

and a test function φ_n such that

$$\begin{aligned} \mathbb{E}_{f_0} \varphi_N &\leq e^{-N r_N^2}, \\ \sup_{f \in \mathcal{F}_N: \rho(f, f_0) > C_2 N r_N^2} \mathbb{E}_f (1 - \varphi_N) &\lesssim e^{-N r_N^2/16}. \end{aligned} \quad (\text{S14})$$

We already proved (S12) in Lemma 2. To verify (S13), we consider the sieve,

$$\mathcal{F}_n = \left\{ (\boldsymbol{\beta}, \sigma, \rho) : 0 < \sigma < e^{C_4 N r_N^2}, e^{-C_4 N r_N^2} < \rho < 1 - e^{-C_4 N r_N^2}, \beta_j \in \mathcal{B}_N^j, j = 0, \dots, p \right\},$$

where for each $j = 0, \dots, p$, \mathcal{B}_N^j is defined as the sieve in the proof of Theorem 7.1 of Ročková and Saha (2019), i.e. the union of all functions belonging to the class of functions \mathcal{F}_ε (defined in Ročková and van der Pas (2019)) that are supported on a valid ensemble \mathcal{VE} (Ročková and van der Pas, 2019), where each tree in the j th ensemble \mathcal{E}_j has at most l_N^j leaves, and l_N^j is chosen as $l_N^j = \lfloor \tilde{D} N (r_N^j)^2 / \log N \rfloor \asymp N^{R/(2\alpha_j+R)}$, for sufficiently large $\tilde{D} > 0$. With this choice of sieve, we have

$$\Pi(\mathcal{F}_n^c) \leq \Pi(\sigma > e^{C_4 N r_N^2}) + \Pi(\rho \leq e^{-C_4 N r_N^2}) + \Pi(\rho \geq 1 - e^{-C_4 N r_N^2}) + \sum_{j=0}^p \Pi(\beta_j \notin \mathcal{B}_n^j). \quad (\text{S15})$$

Since we assumed that $\nu > 1$ in the half- t_ν prior on σ , $\mathbb{E}(\sigma)$ is well-defined, and a simple application of the Markov inequality gives $\Pi(\sigma > e^{C_4 N r_N^2}) \leq e^{-C_4 N r_N^2} \mathbb{E}(\sigma) \lesssim e^{-C_5 N r_N^2}$ for

some $C_5 > 0$. Obviously, the second and third terms in (S15) are each equal to $e^{-C_4 N r_N^2}$, since $\rho \sim \mathcal{U}(0, 1)$.

We now focus on bounding the final term in (S15) from above. Let L_m^j denote the number of terminal leaf nodes in the m th tree of the j th tree ensemble \mathcal{E}_j corresponding to the functional $\beta_j(\mathbf{z})$. Let $l_N^{\min} = \min\{l_N^1, \dots, l_N^p\}$, recalling $l_N^j = \lfloor \tilde{D}N(r_N^j)^2 / \log N \rfloor$. Noting that all the BART priors have the same number of trees M , we have that the second term in (S15) can be bounded above as

$$\begin{aligned}
\sum_{j=0}^p \Pi(\beta_j \notin \mathcal{B}_n^j) &\leq \sum_{j=0}^p \Pi\left(\bigcup_{m=1}^M \{L_m^j > l_N^j\}\right) \\
&\leq \sum_{j=0}^p \sum_{m=1}^M \Pi(L_m^j > l_N^j) \\
&\lesssim M \sum_{j=0}^p e^{-C_l l_N^j \log l_N^j} \\
&\lesssim Mp \exp(-C_l l_N^{\min} \log l_N^{\min}) \\
&= M \exp(\log p - C_l l_N^{\min} \log l_N^{\min}), \tag{S16}
\end{aligned}$$

where we used the proof of Theorem 7.1 of Ročková and Saha (2019) for the third line. By our assumption on the growth rate of p in Assumption (A3), we have $M e^{-C_l l_N^{\min} \log l_N^{\min} + \log p + C_5 N r_N^2} \rightarrow 0$ as $N, p \rightarrow \infty$ for sufficiently large $C_l > 0$ and any $C_5 > 0$. Thus, we have from (S16) that the final term on the right-hand side of (S15) is bounded above by $e^{-C_6 n r_N^2}$ for some $C_6 > 0$. Since each of the terms in (S15) can be bounded above by $e^{K N r_N^2}$ for some constant K , we see that (S13) holds.

Now we show the existence of a test function φ_N so that (S14) also holds. As in Bai et al. (2019), we first consider the most powerful Neyman-Pearson test $\phi_N = \mathbb{I}\{f_1/f_0 \geq 1\}$ for any f_1 such that $\rho(f_0, f_1) \geq N r_N^2$, where $f_1 = \prod_{i=1}^n f_{1,i}$ and $f_{1,i}$ is the density for $\mathbf{y}_i \sim \mathcal{N}_{n_i}(\boldsymbol{\theta}_{1,i}, \sigma_1^2 \boldsymbol{\Sigma}_i(\rho_1))$. If the average Rényi divergence between f_0 and f_1 is bigger than r_N^2 , then

$$\begin{aligned}
\mathbb{E}_{f_0} \phi_N &\leq e^{-N \varepsilon_N^2}, \\
\mathbb{E}_{f_1} (1 - \phi_N) &\leq e^{-N \varepsilon_N^2}. \tag{S17}
\end{aligned}$$

By the Cauchy-Schwarz inequality, we have

$$\mathbb{E}_f (1 - \phi_N) \leq \{\mathbb{E}_{f_1} (1 - \phi_N)\}^{1/2} \{\mathbb{E}_{f_1} (f/f_1)^2\}^{1/2}, \tag{S18}$$

and thus, following from the second inequality in (S17) and (S18), we can control the probability of Type II error properly if $\mathbb{E}_{f_1}(f/f_1)^2 \leq e^{7Nr_N^2/8}$. Using Assumptions (A2) and (A4) and the same arguments as those in the proof of Lemma 2 in Bai et al. (2019), we have that $\mathbb{E}_{f_1}(f/f_1)^2$ is bounded above by $e^{7Nr_N^2/8}$ for densities f_1 satisfying

$$\begin{aligned} \|\boldsymbol{\theta} - \boldsymbol{\theta}_1\|_2^2 &\leq \frac{Nr_N^2}{16}, \\ \frac{1}{n} \|\sigma^2 \boldsymbol{\Sigma}(\rho) - \sigma_1^2 \boldsymbol{\Sigma}(\rho_1)\|_F^2 &\leq \frac{r_N^4}{4n_{\max}^2}. \end{aligned} \quad (\text{S19})$$

Combining this with the second inequality in (S17) and (S18) gives

$$\mathbb{E}_f(1 - \phi_N) \lesssim e^{-Nr_N^2/16}.$$

Thus, we see from the first inequality in (S17) and the above inequality that the test φ_N satisfying (S14) is obtained as the maximum of all tests ϕ_N described above, for each piece required to cover the sieve. To complete the proof of (S14), we need to show that the metric entropy, $\log N(r_N, \mathcal{F}_N, \rho(\cdot))$, i.e. the logarithm of the maximum number of pieces needed to cover \mathcal{F}_N can be bounded above asymptotically by Nr_N^2 . By Assumption (A2), we have that $\frac{1}{N} \|\boldsymbol{\theta} - \boldsymbol{\theta}_1\|_2^2 \leq D_2^2(p+1) \sum_{j=0}^p \|\beta_j - \beta_{0j}\|_N^2$, and by Assumption (A4), the left-hand side of the second inequality in (S19) is bounded above by $n_{\max}^2(\sigma^2 - \sigma_1^2)^2 + e^{2C_4Nr_N^2} n_{\max}^4(\rho - \rho_1)^2$ on $\tilde{\mathcal{F}}_N$. Thus, for densities f_1 satisfying (S19), the metric entropy can be bounded above by

$$\begin{aligned} &\sum_{j=0}^p \log N \left(\frac{r_N}{4D_2\sqrt{p+1}}, \{\beta_j \in \mathcal{F}_N : \|\beta_j - \beta_{0j}\|_N < r_N\}, \|\cdot\|_N \right) \\ &\quad + \log N \left(\frac{r_N^2}{\sqrt{8}n_{\max}^2}, \{\sigma^2 : 0 < \sigma^2 < e^{C_4Nr_N^2}\}, |\cdot| \right) \\ &\quad + \log N \left(\frac{r_N^2}{\sqrt{8}n_{\max}^3 e^{C_4Nr_N^2}}, \{\rho : 0 < \rho < 1\}, |\cdot| \right). \end{aligned} \quad (\text{S20})$$

One can easily verify that the last two terms in (S20) are upper bounded by a constant factor of Nr_N^2 . By modifying the proof of Theorem 7.1 in Ročková and Saha (2019) appropriately, we have for some $A_2 > 0$ and small $\delta > 0$ that the first term in (S20) can be upper bounded by

$$\sum_{j=0}^p \left[(l_N^j + 1)M \log(NRl_N^j) + A_2 M l_N^j \log \left(972D_2 \sqrt{M(p+1)l_N^j N^{1+\delta/2}} \right) \right], \quad (\text{S21})$$

where M is the number of trees in each ensemble \mathcal{B}_N^j . Recalling that M is fixed, $l_N^j \asymp N(r_N^j)^2 / \log N$ where $r_N^j = N^{-\alpha_j/(2\alpha_j+R)} \log^{1/2} N$, and Assumption (A3) that $R = O(\log^{1/2} N)$, we have that each summand in the first term in (S20) is upper bounded by $N(r_N^j)^2$, and so (S21) is asymptotically bounded above by $N \sum_{j=0}^p (r_N^j)^2 = Nr_N^2$. Therefore, from (S20)-(S21), we have for densities f_1 satisfying (S19),

$$\log N(r_N, \mathcal{F}_N, \rho(\cdot)) \lesssim Nr_N^2,$$

and so this completes the proof of (S14). Having established (S12)-(S14), it follows that we have posterior contraction with respect to average Rényi divergence, i.e. (S11) holds. \square

With Lemmas 2 and 3, we now have the ingredients to prove Theorem 1.

Proof of Theorem 1. By Lemma 3, $\Pi(N^{-1}\rho(f, f_0) \lesssim r_N^2 | \mathbf{Y}) \rightarrow 1$ in $\mathbb{P}_{f_0}^{(N)}$ -probability as $N, p \rightarrow \infty$, where $\rho(f_0, f)$ is the Rényi divergence of order 1/2. Under our assumptions and following similar arguments as those in the proof of Lemma 3 in Bai et al. (2019), posterior contraction w.r.t. average Rényi divergence then implies

$$\begin{aligned} r_N^2 &\gtrsim \frac{1}{N} \|\boldsymbol{\theta} - \boldsymbol{\theta}_0\|_2^2 / (1 + r_N^2) \\ &= \frac{1}{N(1 + r_N^2)} \sum_{i=1}^n \sum_{t=1}^{n_i} \left[\sum_{j=0}^p [\beta_j(\mathbf{z}_{ij}) x_{itj} - \beta_{0,j}(\mathbf{z}_{ij}) x_{itj}] \right]^2 \\ &\gtrsim \frac{1}{N(1 + r_N^2)} \sum_{i=1}^n \sum_{t=1}^{n_i} \sum_{j=0}^p (\beta_j(\mathbf{z}_{ij}) - \beta_{0,j}(\mathbf{z}_{ij}))^2 \\ &\asymp \|\boldsymbol{\beta} - \boldsymbol{\beta}_0\|_N^2, \end{aligned} \tag{S22}$$

where we used Assumption (A1) that $\|\beta_j\|_\infty < \infty$ for all $1 \leq j \leq p$ and Assumption (A2) that the covariates x_{itj} , $1 \leq i \leq n$, $1 \leq t \leq n_i$, $1 \leq j \leq p$, are uniformly bounded in the third line of the display. In the final line, we used the fact that $r_N^2 \rightarrow 0$ as $N \rightarrow \infty$. Thus, from (S22), the posterior is asymptotically supported on the event $\{\boldsymbol{\beta} : \|\boldsymbol{\beta} - \boldsymbol{\beta}_0\|_N^2 \leq M_2^2 r_N^2\}$ for sufficiently large N and some large constant $M_2 > 0$. This proves the theorem. \square